Laser induced modifications and waveguides writing inside silicon

by

Xinya Wang

B.S., Nankai University, 2014

AN ABSTRACT OF A DISSERTATION

submitted in partial fulfillment of the requirements for the degree

DOCTOR OF PHILOSOPHY

Department of Industrial and Manufacturing Systems Engineering
Carl R. Ice College of Engineering

KANSAS STATE UNIVERSITY
Manhattan, Kansas

2023

Abstract

Silicon is the basic material for semiconductor industry and laser direct writing in the bulk of silicon has attracted people's attention since 20 years ago. However, the research of laser-matter interaction inside silicon is limited and the formation process of the subsurface modification is not clear enough. In addition, the attempts in the past decade to generate waveguides inside silicon are not satisfactory. Based on this situation, this dissertation has two objectives. The first one is to study the fundamental process of laser-matter interaction and have a better understanding of the material modification process inside silicon, and the second one is to write straight and curved waveguides inside silicon and characterize these waveguides. The first objective will be achieved through a comprehensive experimental study on the physics behind the nanosecond (ns) laser writing process. The experimental study will involve generating subsurface modifications inside silicon and characterize the modifications by optical microscopy, SEM, TEM, and Raman spectroscopy. The second objective will be achieved through laser transverse writing and by shaping the laser beam through a pair of cylindrical lenses and focusing the shaped beam inside the silicon.

It is found that permanent modifications are made with tightly focused ns pulses at 1.55 μm wavelength inside silicon without damaging the front surface. Examinations of the modified zone using Raman spectroscopy and TEM reveal a disturbed crystal structure with defects and strained areas. For the first time, high resolution TEM images show a direct evidence of amorphous silicon inside ns laser induced modifications. A quantitative analysis based on Raman spectra of the modified zone indicates that the amorphous silicon accounts for only a small percentage of the total modification. More work is needed to determine the effects of laser parameters on the amorphous transition inside silicon. Nanosecond laser transverse writing of

different types of waveguides inside silicon are demonstrated, such as straight waveguides, curved waveguides with different radii, and straight-curved waveguides. A nearly circular transverse guide-profile is formed with the shaped beam. The waveguides are found to support single-mode propagation for 1.55 μm wavelength light. The loss is found to be about 3 dB/cm for straight waveguide and can be larger for curved waveguides depending on the curvature. The knowledge gained from this research will enable us to have a better understanding of laser-matter interaction inside silicon and pave the way for its future applications in the semiconductor field.

Laser induced modifications and waveguides writing inside silicon

by

Xinya Wang

B.S., Nankai University, 2014

A DISSERTATION

submitted in partial fulfillment of the requirements for the degree

DOCTOR OF PHILOSOPHY

Department of Industrial and Manufacturing Systems Engineering
Carl R. Ice College of Engineering

KANSAS STATE UNIVERSITY
Manhattan, Kansas

2023

Approved by:

Major Professor
Dr. Shuting Lei

Copyright

Abstract

Silicon is the basic material for semiconductor industry and laser direct writing in the bulk of silicon has attracted people's attention since 20 years ago. However, the research of laser-matter interaction inside silicon is limited and the formation process of the subsurface modification is not clear enough. In addition, the attempts in the past decade to generate waveguides inside silicon are not satisfactory. Based on this situation, this dissertation has two objectives. The first one is to study the fundamental process of laser-matter interaction and have a better understanding of the material modification process inside silicon, and the second one is to write straight and curved waveguides inside silicon and characterize these waveguides. The first objective will be achieved through a comprehensive experimental study on the physics behind the nanosecond (ns) laser writing process. The experimental study will involve generating subsurface modifications inside silicon and characterize the modifications by optical microscopy, SEM, TEM, and Raman spectroscopy. The second objective will be achieved through laser transverse writing and by shaping the laser beam through a pair of cylindrical lenses and focusing the shaped beam inside the silicon.

It is found that permanent modifications are made with tightly focused ns pulses at 1.55 μm wavelength inside silicon without damaging the front surface. Examinations of the modified zone using Raman spectroscopy and TEM reveal a disturbed crystal structure with defects and strained areas. For the first time, high resolution TEM images show a direct evidence of amorphous silicon inside ns laser induced modifications. A quantitative analysis based on Raman spectra of the modified zone indicates that the amorphous silicon accounts for only a small percentage of the total modification. More work is needed to determine the effects of laser parameters on the amorphous transition inside silicon. Nanosecond laser transverse writing of

different types of waveguides inside silicon are demonstrated, such as straight waveguides, curved waveguides with different radii, and straight-curved waveguides. A nearly circular transverse guide-profile is formed with the shaped beam. The waveguides are found to support single-mode propagation for 1.55 μm wavelength light. The loss is found to be about 3 dB/cm for straight waveguide and can be larger for curved waveguides depending on the curvature. The knowledge gained from this research will enable us to have a better understanding of laser-matter interaction inside silicon and pave the way for its future applications in the semiconductor field.

Table of Contents

List of Figures

List of Tables

Acknowledgements

First of all, I would like to sincerely thank my advisor Professor Shuting Lei for giving me the opportunity to be his student. I'm grateful for his supporting and guidance during my graduate studies at K-state. He taught and encouraged me to how to question thought and express ideas through research process. His brilliant ideas, patience and expertise help me overcome setbacks and stay focused on my graduate study.

Special thanks also go to Dr. Xiaoming Yu for giving me training in my first year of PhD and for his constant support and guidance. He provided lots of valuable suggestions on my research. His expertise and knowledge in optical and laser field were paramount in providing a well-rounded experience consistent my long-term career goals.

I would like to thank to Dr. Matthew Berg for his useful suggestions and kind advices on my research. His advice about research approaches will benefit my academic career. I also thank Dr. Meng Zhang and Supreme Das for serving as a chair of my committee and conducting the final defense exam. And I would like to thank the strong support from our department head Professor Bradley A. Kramer. I would also like to acknowledge the faculty and staff of our department for offering me with a tremendous graduate education. They have taught me how to think about industrial engineering and scientific problems and provided me with the foundation for becoming a well-training engineer or scientist. Thank Dr. Shing I Chang, Dr. John Wu for their help.

Majority of the research was conducted in the James R. MacDonald Laboratory, Department of Physics at KSU. I would like to thank all the professors and staff who gave me selfless assistance with my research and took the responsibility of maintaining the equipment.

This dissertation would be impossible to finish without assistance from postdocs and fellow students from and outside of our group. I would like to thank Yang Yang, Guang Yang, Kaiming Bi, Yuyang Chen, Pingping Chen, Ruqi Chen, Mingman Sun, Sajed Hosseini-Zavareh, HongyuShi, Lianjie Xue, Huynh Lam, Tomthin Nganba Wangjam, Lanh Trinh, Mohammad Najjartabar Bisheh, Keren Zhao, Marzieh Soltanolkottabi, Pedram Parandoush, Kasun Fernando, Sogand Sabahfar, etc.

Thank my parents and my wife.

Chapter 1 - Introduction

1. Background

Silicon is the basic semiconductor material for numerous applications, such as photovoltaics, sensors, and microelectronics. In the 1970s, the empirical Moore's law predicted that the size of transistors should be comparable to one of the atoms in the 2020s. The latest improvements in quantum computing are expected to achieve this milestone [1]. These advancements are related to the extraordinary development of "silicon-on-insulator" (SOI) lithography that allows the fabrication of functional micro- and nanodevices for guiding, modulating, emitting, and detecting light in silicon [2-4].

However, SOI technology has several constraints. First, to fabricate 3D architectures, one needs to do the layer-by-layer deposition; second, an extremely clean environment is necessary; and finally, it often takes plenty of time to do the fabrication. Laser direct writing in the bulk of silicon has been an attractive alternative for the SOI technique since 1996 [5-7]. In the following 20 years, numerous researchers have put effort on the study of interaction between laser and silicon [8-10].

The theoretical and experimental work in [11-15] has revealed the basic physical processes that govern the laser-silicon interaction. This novel understanding subsequently provided multiple possibilities for making new devices within silicon [16-23]. As one example, 3D laser writing in the bulk of silicon has led to inscriptions of many functions including waveguides, data storage, holograms, microfluidic channels, gratings, and surface textures [19-28]. Achievements like these mark the beginning of a new era of laser. Nowadays, the next generation of μJ-class mid-infrared lasers have been a reality [29,30]. The new lasers definitely provide more possibilities for studying this topic [31].

Despite the success over the past years, 3D laser writing to generate functional modifications inside silicon is still far behind what has been achieved with dielectrics. Therefore, significant amount of work is needed to advance the fundamental understanding of 3D laser writing inside

silicon and to realize its full technological potential. In the following, an overview of the literature in laser modification and waveguide writing inside silicon will be made, which will lead to the proposed research.

2. Literature Review

Laser-induced subsurface modifications inside silicon is a well-known phenomenon [11,19]. The subsurface modification technology is based on tightly focusing short laser pulses inside the bulk of silicon, thereby creating localized changes to its crystal structure [21]. One of the most successful applications of subsurface modifications in silicon is dry and nearly debris-free wafer dicing [32, 33]. Since silicon is the material of choice for the semiconductor industry, it is of great interest to further develop the subsurface modification technology for silicon. Previous work reports two-photon–induced subsurface modification of Si using an erbium-doped fiber laser pulsed at 3.5 ns [16]. The crystal structure of the laser induced subsurface modifications in Si is presented in [21]. Investigations of the properties of the subsurface modifications generated by ns laser pulses can be found in [39]. Local modification in bulk Si with sub-100-fs laser pulses is achieved in [18] with single pulses tightly focused at the center of silicon spheres using extreme solid-immersion focusing. A wide variety of material changes inside silicon induced by pulsed laser were discovered, including voids [34,35], high pressure phases [36], dislocations [27,28,37,38], hydrostatic compressive strain [27,28,37,38], cracks [22], amorphous silicon [21], as well as polycrystalline features [6,19].

One attracting application of the laser induced subsurface modifications is writing waveguides inside silicon [20,24]. Generally speaking, the application is based on laser-induced structural modifications that manifest a refractive-index contrast with the surrounding unmodified regions inside silicon [24]. Despite the importance of silicon (Si) in the microelectronics industry and its growing importance in photonics, studies on waveguide writing in this material are limited. Depressed-cladding waveguides inside bulk silicon written by ns laser pulses are achieved in [26]. Waveguides can also be written using femtosecond (fs) pulses as demonstrated in [11], even though the induced modifications are generated only at the SiO_2/Si interface. Waveguides deep into bulk Si are first reported with 350 fs laser pulses at a wavelength of 1550 nm in [19,20] where a 10^{-4} refractive-index change in magnitude is seen.

In general, two methods can be used to write waveguides in Si: longitudinal and transverse [40]. The advantage of the longitudinal writing is that the waveguides have a symmetric cross section; however, the waveguide length is limited by the objective-lens focal length [40]. In the transvers writing, the waveguide length is not restricted by the working distance of the objective lens, but the waveguide profile takes an asymmetric droplet-like shape [40]. An advantage of the transverse writing method is that it provides more flexibility for writing waveguide paths with complex shapes, i.e., shapes other than linear paths. Semicircular, or curved, waveguide paths are one example. The theory of bending loss in curved waveguides is established in [41-45].

In summary, the past decades have seen some achievements in the field of laser induced modifications and waveguide writing inside silicon; however, many problems remain to be solved. The first problem is related to the difficulty to produce uniform modifications inside silicon induced by a pulsed laser. When laser pulses are focusing inside the silicon, the extreme high temperature and pressure at the focusing spot often result in complicated material change, such as melting, microexplosion, re-solidification and phase change [46]. A fundamental study of this process is essential for the development of high performance silicon devices. The second problem is how to overcome the drawback of the short working distance of an objective lens and to write long waveguides inside silicon. The third one is that the shape of the focusing spot is often droplet like in transverse writing, and the effect is stronger considering the high refractive index of silicon (~3.5). The resulted elongated cross section shape of the waveguides should be avoided through beam shaping.

3. Research Objective

This dissertation tries to answer this question: How can we take advantage of the laser to make modifications inside silicon and how to extend the modifications into meaningful devices such as waveguides? This question is approached from various angles: What are the modifications inside silicon? What are the properties of the modifications? What is the formation process of the modifications? Can we control the structure of the modifications? Is it possible to write waveguides inside silicon? If yes, what is the performance of the waveguide? Can we reduce the loss of the waveguides? Can we make waveguides besides straight shapes?

The research objective is twofold. The first objective is to study the fundamental process of the laser-matter interaction and have a better understanding of the material change inside silicon. The second objective is to write straight and curved waveguides inside silicon and characterize these waveguides and extend to more complicated shapes.

4. Outline of the dissertation

The dissertation is organized as follows.

Chapter 1 constitutes background information, a literature review, and the research objectives.

Chapter 2 presents the work on the characterization and control of laser induced modification inside silicon.

Chapters 3 and 4 present the work on the waveguide writing inside silicon.

Chapter 5 presents the work on the complex waveguides writing inside silicon.

Chapter 6 presents the work on the structural changes of nanosecond laser modification inside silicon.

Chapter 7 is the summary and outlook.

References

[1] Arute, Frank, Kunal Arya, Ryan Babbush, Dave Bacon, Joseph C. Bardin, Rami Barends, Rupak Biswas et al. "Quantum supremacy using a programmable superconducting processor." *Nature* 574, no. 7779 (2019): 505-510.

[2] Lipson, Michal. "Guiding, modulating, and emitting light on silicon-challenges and opportunities." *Journal of Lightwave Technology* 23, no. 12 (2005): 4222.

[3] Foster, Mark A., Amy C. Turner, Jay E. Sharping, Bradley S. Schmidt, Michal Lipson, and Alexander L. Gaeta. "Broad-band optical parametric gain on a silicon photonic chip." *Nature* 441, no. 7096 (2006): 960-963.

[4] Foster, Mark A., Reza Salem, David F. Geraghty, Amy C. Turner-Foster, Michal Lipson, and Alexander L. Gaeta. "Silicon-chip-based ultrafast optical oscilloscope." *Nature* 456, no. 7218 (2008): 81-84.
[5] Davis, K. Miura, Kiyotaka Miura, Naoki Sugimoto, and Kazuyuki Hirao. "Writing waveguides in glass with a femtosecond laser." *Optics letters* 21, no. 21 (1996): 1729-1731.
[6] Chambonneau, Maxime, David Grojo, Onur Tokel, Fatih Ömer Ilday, Stelios Tzortzakis, and Stefan Nolte. "In-Volume Laser Direct Writing of Silicon—Challenges and Opportunities." *Laser & Photonics Reviews* 15, no. 11 (2021): 2100140.
[7] Miura, K., Jianrong Qiu, H. Inouye, T. Mitsuyu, and K. Hirao. "Photowritten optical waveguides in various glasses with ultrashort pulse laser." Applied Physics Letters 71, no. 23 (1997): 3329-3331.
[8] Soref, Richard. "Mid-infrared photonics in silicon and germanium." *Nature photonics* 4, no. 8 (2010): 495-497.
[9] Hochberg, Michael, and Tom Baehr-Jones. "Towards fabless silicon photonics." *Nature photonics* 4, no. 8 (2010): 492-494.
[10] Koehl, Sean, Ansheng Liu, and Mario Paniccia. "Integrated silicon photonics: Harnessing the data explosion." *Optics and Photonics News* 22, no. 3 (2011): 24-29.
[11] Nejadmalayeri, Amir H., Peter R. Herman, Jonas Burghoff, Matthias Will, Stefan Nolte, and Andreas Tünnermann. "Inscription of optical waveguides in crystalline silicon by mid-infrared femtosecond laser pulses." *Optics Letters* 30, no. 9 (2005): 964-966.
[12] Crawford, T. H. R., J. Yamanaka, G. A. Botton, and H. K. Haugen. "High-resolution observations of an amorphous layer and subsurface damage formed by femtosecond laser irradiation of silicon." *Journal of Applied Physics* 103, no. 5 (2008): 053104.
[13] Mouskeftaras, Alexandros, Andrei V. Rode, Raphaël Clady, Marc Sentis, Olivier Utéza, and David Grojo. "Self-limited underdense microplasmas in bulk silicon induced by ultrashort laser pulses." *Applied Physics Letters* 105, no. 19 (2014): 191103.
[14] Zavedeev, E. V., V. V. Kononenko, V. M. Gololobov, and V. I. Konov. "Modeling the effect of fs light delocalization in Si bulk." *Laser Physics Letters* 11, no. 3 (2014): 036002.
[15] Fedorov, V. Yu, M. Chanal, D. Grojo, and S. Tzortzakis. "Accessing extreme spatiotemporal localization of high-power laser radiation through transformation optics and scalar wave equations." Physical review letters 117, no. 4 (2016): 043902.

[16] Verburg, P. C., G. R. B. E. Römer, and A. J. Huis. "Two-photon–induced internal modification of silicon by erbium-doped fiber laser." *Optics express* 22, no. 18 (2014): 21958-21971.
[17] Mori, Masahiro, Yasuhiko Shimotsuma, Tomoaki Sei, Masaaki Sakakura, Kiyotaka Miura, and Haruhiko Udono. "Tailoring thermoelectric properties of nanostructured crystal silicon fabricated by infrared femtosecond laser direct writing." *physica status solidi (a)* 212, no. 4 (2015): 715-721.
[18] Chanal, Margaux, Vladimir Yu Fedorov, Maxime Chambonneau, Raphaël Clady, Stelios Tzortzakis, and David Grojo. "Crossing the threshold of ultrafast laser writing in bulk silicon." *Nature communications* 8, no. 1 (2017): 1-6.
[19] Tokel, Onur, Ahmet Turnalı, Ghaith Makey, Parviz Elahi, Tahir Çolakoğlu, Emre Ergeçen, Özgün Yavuz et al. "In-chip microstructures and photonic devices fabricated by nonlinear laser lithography deep inside silicon." *Nature photonics* 11, no. 10 (2017): 639-645.
[20] Pavlov, I. H. O. R., O. Tokel, S. Pavlova, V. Kadan, G. Makey, A. Turnali, Ö. Yavuz, and F. Ö. Ilday. "Femtosecond laser written waveguides deep inside silicon." *Optics Letters* 42, no. 15 (2017): 3028-3031.
[21] Verburg, P. C., L. A. Smillie, G. R. B. E. Römer, Bianca Haberl, J. E. Bradby, J. S. Williams, and A. J. Huis. "Crystal structure of laser-induced subsurface modifications in Si." *Applied Physics A* 120, no. 2 (2015): 683-691.
[22] Iwata, Hiroyuki, Daisuke Kawaguchi, and Hiroyasu Saka. "Electron microscopy of voids in Si formed by permeable pulse laser irradiation." *Microscopy* 66, no. 5 (2017): 328-336.
[23] Kämmer, Helena, Gabor Matthäus, Kim A. Lammers, Christian Vetter, Maxime Chambonneau, and Stefan Nolte. "Origin of waveguiding in ultrashort pulse structured silicon." *Laser & Photonics Reviews* 13, no. 2 (2019): 1800268.
[24] Chambonneau, M., Q. Li, M. Chanal, N. Sanner, and D. Grojo. "Writing waveguides inside monolithic crystalline silicon with nanosecond laser pulses." *Optics letters* 41, no. 21 (2016): 4875-4878.
[25] Matthäus, G., H. Kämmer, K. A. Lammers, C. Vetter, W. Watanabe, and S. Nolte. "Inscription of silicon waveguides using picosecond pulses." *Optics express* 26, no. 18 (2018): 24089-24097.

[26] Turnali, Ahmet, Mertcan Han, and Onur Tokel. "Laser-written depressed-cladding waveguides deep inside bulk silicon." *JOSA B* 36, no. 4 (2019): 966-970.
[27] Chambonneau, M., D. Richter, S. Nolte, and D. Grojo. "Inscribing diffraction gratings in bulk silicon with nanosecond laser pulses." *Optics letters* 43, no. 24 (2018): 6069-6072.
[28] Chambonneau, M., X. Wang, X. Yu, Q. Li, D. Chaudanson, S. Lei, and D. Grojo. "Positive- and negative-tone structuring of crystalline silicon by laser-assisted chemical etching." *Optics letters* 44, no. 7 (2019): 1619-1622.
[29] Stutzki, Fabian, Christian Gaida, Martin Gebhardt, Florian Jansen, Andreas Wienke, Uwe Zeitner, Frank Fuchs et al. "152 W average power Tm-doped fiber CPA system." *Optics letters* 39, no. 16 (2014): 4671-4674.
[30] Gaponov, Dmitry, Laure Lavoute, Sébastien Fevrier, A. Hideur, and Nicolas Ducros. "2µm all-fiber dissipative soliton master oscillator power amplifier." In *Fiber Lasers XIII: Technology, Systems, and Applications*, vol. 9728, p. 972834. International Society for Optics and Photonics, 2016.
[31] Chambonneau, M., L. Lavoute, D. Gaponov, V. Yu Fedorov, A. Hideur, S. Février, S. Tzortzakis, O. Utéza, and D. Grojo. "Competing nonlinear delocalization of light for laser inscription inside silicon with a 2-µm picosecond laser." *Physical Review Applied* 12, no. 2 (2019): 024009.
[32] F. Fukuyo, K. Fukumitsu and N. Uchiyama (2005) The Stealth Dicing Technologies and Their Application, Proceedings of 6th Laser Precision Microfabrication.

[33] Izawa, Y., Y. Tsurumi, N. Miyanaga, S. Tanaka, H. Kikuchi, M. Esashi, and M. Fujita. "Debris-free in-air laser dicing for multi-layer MEMS by perforated internal transformation and thermally-induced crack propagation." In *2008 IEEE 21st International Conference on Micro Electro Mechanical Systems*, pp. 822-827. IEEE, 2008.

[34] Iwata, Hiroyuki, Daisuke Kawaguchi, and Hiroyasu Saka. "Electron microscopy of voids in Si formed by permeable pulse laser irradiation." Microscopy 66, no. 5 (2017): 328-336.
[35] Shimamura, K., J. Okuma, S. Ohmura, and F. Shimojo. "Molecular-dynamics study of void-formation inside silicon wafers in stealth dicing." In *Journal of Physics: Conference Series*, vol. 402, no. 1, p. 012044. IOP Publishing, 2012.

[36] Iwata, Hiroyuki, Daisuke Kawaguchi, and Hiroyasu Saka. "Crystal structures of high-pressure phases formed in Si by laser irradiation." *Microscopy* 67, no. 1 (2018): 30-36.
[37] Saka, Hiroyasu, Hiroyuki Iwata, and Daisuke Kawaguchi. "Thermal stability of laser-induced modified volumes in Si as studied by in situ and ex situ heating experiments." *Microscopy* 67, no. 2 (2018): 112-120.
[38] Kawaguchi, Daisuke, Hiroyuki Iwata, and Hiroyasu Saka. "Whereabouts of missing atoms in a laser-injected Si: Part 1." Philosophical Magazine 99, no. 15 (2019): 1849-1865.
[39] Yu, Xiaoming, Xinya Wang, Margaux Chanal, Carlos A. Trallero-Herrero, David Grojo, and Shuting Lei. "Internal modification of intrinsic and doped silicon using infrared nanosecond laser." *Applied Physics A* 122, no. 12 (2016): 1-7.
[40] M. Beresna, M. Gecevicius, and P. G. Kazansky, “Ultrafast laser direct writing and nanostructuring in transparent materials,” Adv. Opt. Photonics 6(3), 293–339 (2014).
[41] Marcuse, Dietrich. "Curvature loss formula for optical fibers." JOSA 66, no. 3 (1976): 216-220.
[42] Marcuse, Dietrich. "Bend loss of slab and fiber modes computed with diffraction theory." *IEEE Journal of Quantum Electronics* 29, no. 12 (1993): 2957-2961.
[43] Lewin, Leonard. "Theory of waveguides: Techniques for the solution of waveguide problems." *New York* (1975).
[44] Lewin, Leonard, David C. Chang, and Edward F. Kuester. "Electromagnetic waves and curved structures." *Stevenage* 2 (1977).
[45] A. Yariv and Y. Pochi Photonics: optical electronics in modern communications (Oxford University, 2006).

Chapter 2 - Characterization and Control of Laser Induced Modification Inside Silicon

This work was published in the paper "Characterization and control of laser induced modification inside silicon," Xinya Wang, Xiaoming Yu, Hongyu Shi, Xianhua Tian, Maxime Chambonneau, David Grojo, Brett Depaola, Matthew Berg, Shuting Lei, Journal of Laser Applications 31 (2), 022601

Abstract

Internal modification of silicon is important for wafer stealth dicing. In this paper, we report experimental and simulation results of three-dimensional (3D) modification inside silicon wafers using laser pulses with 1.55 μm wavelength and 3.5 ns pulse duration. Permanent modification is generated inside silicon by tightly focusing and continuously scanning the laser beam inside samples, without damaging the front and back surface. Cross sections of these modifications are observed after cleaving the samples and are further analyzed after mechanical polishing followed by chemical etching. The shape of the modification is found to depend on the input beam shape, laser power, and scanning speed. With proper conditions, nearly circular modification is obtained, which has potential application for waveguide writing inside silicon.

1 Introduction

When high-intensity laser pulses are focused inside a wafer, each laser pulse results in the production of a subsurface modification. After laser processing, applying tensile stress perpendicularly to this modified-layer, silicon wafer can be separated easily into individual chip without creating any damage to the wafer surface comparing with the conventional blade dicing method. This technology is called "stealth dicing" (SD), and is attracting attentions as a novel dicing technology in semiconductor industries.

The dicing saw is used in conventional dicing of Si wafer. The wafer could be contaminated since this is wet process [1-6]. Besides, large transverse intensity will cause chipping and

microcracks in cut end-faces [7]. Moreover, laser ablation [8, 9] or laser thermal breaking have also been used to do dicing [10,11]. The disadvantage of this method is that it will generate heat and debris pollution and affect device property and reliability. In addition, laser ablation generates microcracks and laser thermal breaking results in low end face accuracy. As for the SD method, there is no damage at the surface layer of a wafer where actual devices are formed. There is no debris contamination and thermal effect. Several groups have reported modifications by pulsed laser inside silicon [12-14]. The relevance of SD to meet the highest possible performance in dicing is a strong motivation to study in detail the formation process of subsurface modifications.

In this paper, we investigate the formation of modification inside intrinsic silicon wafers. The wavelength of the fiber laser in this study is 1.55 μm and the pulse duration is 3.5 ns. By tightly focusing the laser beam with spherical aberration (SA) correction, we write continuous lines inside the samples and analyze their cross sections. The shape of subsurface modification is found to depend on the laser pulse energy, scanning speed, repetition rate and input beam shape. This work provides information for future development of stealth dicing technologies.

2 **Experimental Details**

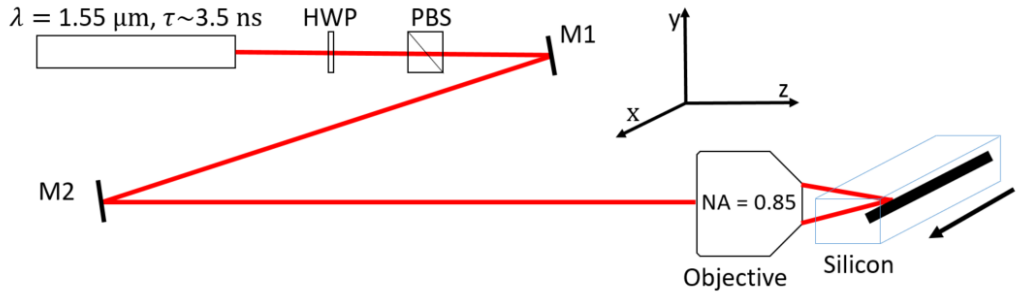

Fig. 1. Experimental setup. M1 and M2 are gold mirrors. HWP and PBS are half-wave plate and polarizing beam splitter, respectively.

The experimental arrangement is depicted in Fig. 1. The samples used in this study are (100)-oriented, 1-mm thick intrinsic silicon wafers. The intrinsic samples have a resistivity of >200 Ω·cm. The laser source (MWTech, PFL-1550) generates pulses at 1550 nm wavelength, and is operated at various repetition rates ranging from 20 to 150 kHz. The pulse duration is τ = 3.5 ns (full width at half-maximum). The maximum pulse energy is 20 μJ. The output beam is

collimated and has a 1/e2 diameter of 6 mm. The beam is focused with an infrared objective lens (NA = 0.85, Olympus, Model LCPLN100XIR), which has SA correction for silicon thickness between 0 and 1 mm (adjustable). At the focus, the beam is spatially Gaussian-shaped with a theoretical diameter at 1⁄e^2 of 〖2w〗_0=1.22 λ⁄(NA=2.2 μm) with Rayleigh lengths z_R(air) = 2.6 μm and z_R (Si) ≈ 9.2 μm in air and silicon, respectively. The wafers are cleaved into small pieces of about 20×20 mm2, which are mounted on a motorized XYZ stage (Newport, Model ILS100PP). The focal depth is controlled by moving the sample along the laser beam's axial direction, and modification is induced by scanning the sample transversely at a constant speed. The focus on the front surface is determined when white-light plasma radiation from surface damage is observed, and the desired depth (d) is reached by moving the sample towards the objective by d/n, where n = 3.5 is the refractive index of silicon at 1.55 μm. The sample after laser writing is cleaved perpendicularly to the scanning direction and the cross sections (in the (110)-plane) are observed with a visible-light optical microscope. The cleaved surface is then polished and examined with the microscope again. The polished surface is put in a 50 wt. % KOH solution and etched for 5 minutes in an ultrasonic bath. Then the sample is observed with the microscope. In this study, damage is not observed on either front or back surface of the silicon samples. Here, the term "modification" refers to any permanent change in the sample after laser treatment, and "damage" refers to significant modification, such as cracks and voids.

3. Results and discussion

3.1. Optimal focal depth with spherical aberration (SA) correction

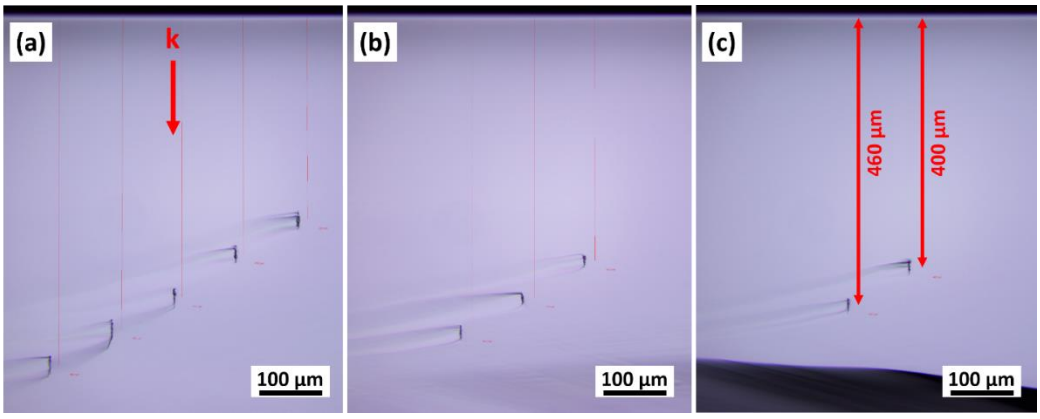

Fig. 2. Cross sections of modification lines in silicon at various depths with pulse energy of (a) 2.0 μJ, (b) 1.5 μJ, and (c) 1.0 μJ. The focusing lens is corrected for spherical aberrations at a depth of

0.5 mm inside silicon (correction collar). Regions in black color and aligned vertically are laser-induced modification. Narrow vertical lines in red color are depth measurements.

Since the difference in refractive index between air and silicon is large, and the beam is focused deep inside the material which extremely increases the spherical aberration, it is necessary to correct spherical aberration. The objective lens used in this study has a correction collar and can compensate aberration in silicon with thickness up to 1 mm. To facilitate later characterization of induced modification, modification is generated in the middle of the samples, and therefore the correction collar is set at 0.5 mm throughout the experiments. However, setting the correction at 0.5 mm does not guarantee optimal focusing at this depth (shown below), since the lens might be designed for a wavelength different from our laser wavelength. To get this optimal focusing depth, continuous lines are made at various depths with 50 µm increments, at a constant speed of 1 mm/s. The samples are then cleaved perpendicularly to the writing direction, and the cross sections are examined with a visible-light microscope. Fig. 2 shows the results for three pulse energies. Regions in black color and aligned vertically are laser-induced modification, and the structures seen outside these regions are caused by the cleaving procedure. Modification is observed within a wider depth range, from 350 to 550 µm, when the pulse energy is 2.0 µJ. When the energy is reduced to 1.0 µJ, only two modifications at 400 and 460 µm can be observed. No modification is seen when the pulse energy is reduced to 0.4 µJ, in very good agreement with similar experiments performed with analogous laser facilities [13, 14].

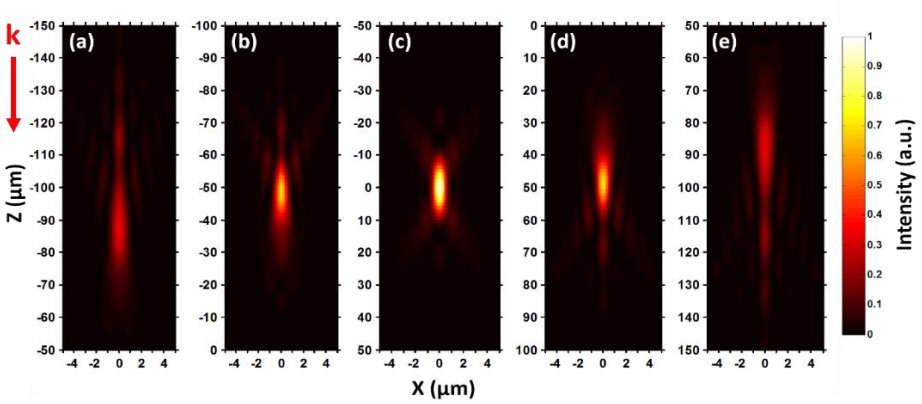

Fig. 3. Calculated focal intensities at various depths inside silicon with the consideration of refractive index mismatch. $Z = 0$ corresponds to a depth of 430 µm. The intended focal depths

are Z = -100, -50, 0, 50 and 100 μm for (a)-(e), respectively. Intensities in all the images are normalized to the peak intensity in (c).

To understand the results in Fig. 2, we calculate the focal shape at various depths, with the consideration of refractive index mismatch. We use the PSF Lab software [18] to obtain focal intensity profiles. The objective lens is assumed to be perfectly corrected for 430 μm thick silicon, and intensities at various depths are calculated, as shown in Fig. 3. We can see that at the depth corresponding to the correction depth (430 μm), the focus is a diffraction-limited spot size consistent with estimation (Fig. 3(c)). When the foci are shifted by about 50 μm ((b) and (d)), the foci are elongated and the peak intensities drop to about 70% of the peak intensity in (c). Further shifting the depth causes even longer foci and lower (35%) peak intensities. This shows that a shift in depth as small as 50 μm can cause reduction of peak intensities and as a consequence disappearance of laser-induced modification, in consistence with the experimental results shown in Fig. 2. We put the laser focus in the optimal depth range of 400 to 460 μm in the following experiments.

3.2. Observation of modification after polishing and KOH etching

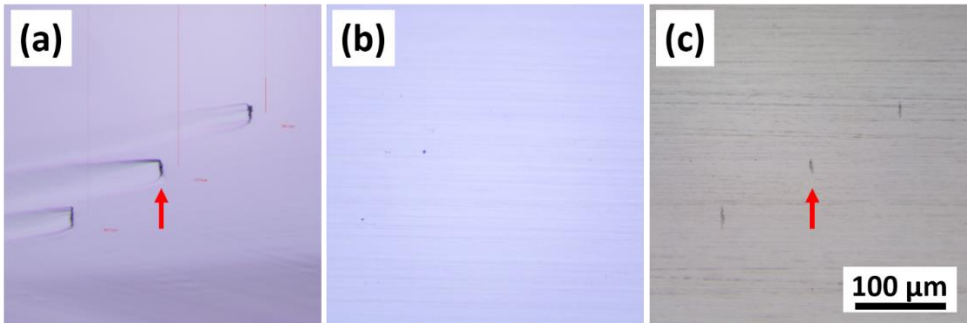

Fig. 4. Cross sections of laser-modified regions after (a) cleaving, (b) polishing, and (c) chemical etching. The laser light is from top to bottom.

Some groups[14-16] directly observe modifications in the bulk. Here, we choose to observe the modification by cleaving the sample, without the limitation in terms of resolution of infrared microscopy. A drawback of this method is that it induces undesired alteration to the samples

(Fig. 2). This might be indistinguishable from the modification caused solely by the laser. To avoid confusion, we apply the polishing-and-etching method that is commonly used in the study for dielectrics [21] and has also been used for silicon recently [18]. The sample from the previous experiment (Fig. 2(b), also shown in Fig. 4(a)) is mechanically polished. Interestingly, the modified regions completely disappear after polishing, as shown in Fig. 4(b). A similar behavior is also reported for femtosecond laser writing [15]. For the samples machined by the highest pulse energy (3.75 μJ) and a much slower scanning speed (0.01 mm/s), modification also disappears after polishing (results not shown here). These findings suggest that the laser-induced modification in this study might merely be local change of density [15], not significant damage such as cracks and voids, because otherwise one would expect to see some type of irregularities on the polished surface. The change of density manifests itself after the disturbance during the sample cleaving procedure, and therefore modified regions can be observed in Fig. 4(a). After polishing, we etch the sample by 50 wt.% KOH solution for 5 minutes in an ultrasonic bath. The laser-modified regions reappear as shown in Fig. 4. Meanwhile, the alteration caused by cleaving is absent. Similar etching selectivity is reported in dielectrics [22].

3.3. Morphology of resultant modification

3.3.1 The influence of pulse energy on modification morphologies

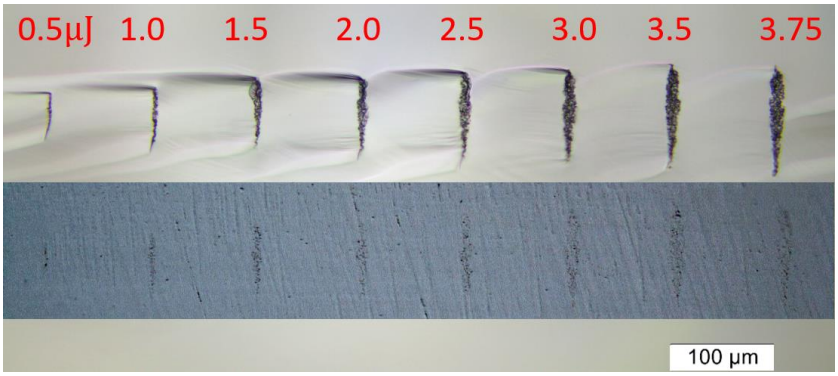

Fig. 5. Laser-induced modification at the same depth (430 μm) and with increasing pulse energy (Upper row is after cleaving, and lower row is after polishing and etching). Numbers above the

modified regions represent pulse energy in µJ. The scanning speed is 1mm/s. The laser light is from top to bottom.

The absorption of 1.55 µm wavelength light in silicon is a two-photon absorption process. The nature of absorption is complicated since the difference between the photon energy (0.8 eV) and the bandgap (1.1 eV) is small. Previous work shows that the heating of silicon by the laser may cause the bandgap to shrink, leading to linear absorption [16]. Therefore, it is necessary to quantify the size and volume of the absorption regions.

For this purpose, we focus the beam at a fixed depth of 430 µm and write lines with increasing pulse energy. The cross sections treated after the polishing-etching procedure are shown in Fig. 5. As expected, the modifications become larger with increasing pulse energy. The shape of modification is an inverse triangle when the pulse energy is high. We make a simple estimate and find that the energy density in the modified volume is between 0.5 to 4.6 kJ/cm^3, orders-of-magnitude below the damage threshold (MJ/cm^3 in glass) for cracks and voids. While using high-order photo-ionization from longer wavelengths can achieve tighter focusing, other mechanisms, such as plasma defocusing [20], might impair the effectiveness in realizing high energy density. It is critical to understand the fundamental mechanisms in the laser-energy deposition process in order to further improve the stealth dicing technique.

3.3.2 The influence of laser scanning speed on modification morphologies

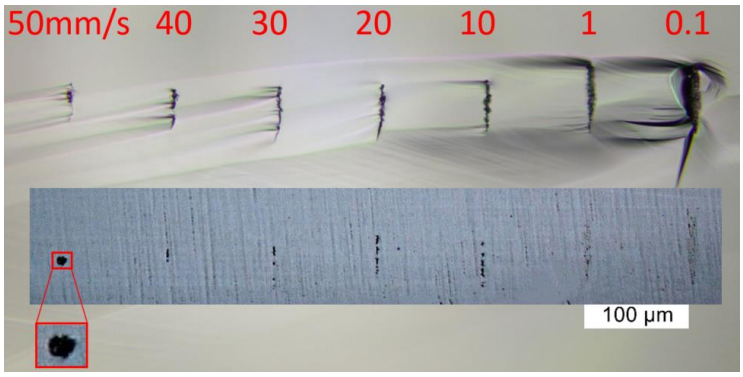

Fig. 6. Modifications at various scanning speed (Upper row is after cleaving, and lower row is after polishing and etching). Pulse energy is 1.5 µJ and repetition rate is 20 kHz. The laser light is from top to bottom.

Laser scanning speed affects the modification morphologies at the same energy density since the speed is related to the number of pulses absorbed by the material based on the equation N=RS/V, where N is the pulse number, R the pulse repetition rate, S the beam focal spot size and V the laser scanning speed [23].

With fixed pulse energy, repetition rate and focal spot size, the scanning speed is the only parameter that can be varied in order to control the modification shape. Modification length and width at various scanning speeds are shown in Fig. 6. At a low speed (0.1 mm/s), we can observe the modification with the width of 12.5 µm and 68.9 µm, respectively. In particular, at the speed of 10-30 mm/s, the modifications break to several parts. Furthermore, with the speed increasing to 50 mm/s, the modification is almost circular (the length and width are 8.9 µm and 11.3 µm, respectively), which has potential application for waveguide writing inside silicon. Therefore, we can tune the scanning speed to control the modification length and width.

3.3.3 The influence of repetition rate on modification

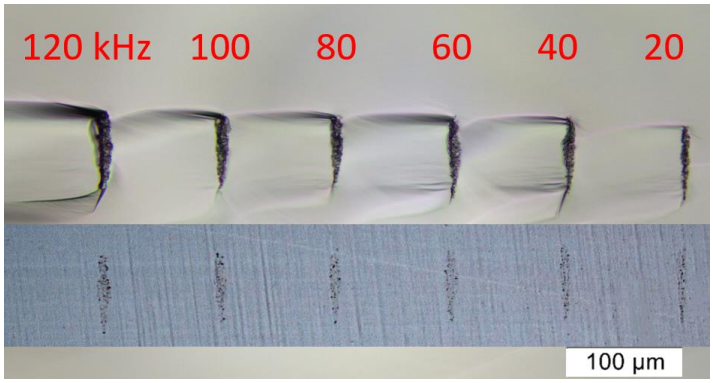

Fig. 7. Modifications at various repetition rate (Upper row is after cleaving, and lower row is after polishing and etching). The pulse energy is 1.5 µJ and the scanning speed is 1 mm/s. The laser light is from top to bottom.

With fixed scanning speed, pulse energy and focal spot size, the repetition rate affects the modification shape.

In Fig. 7, scanning speed is set to 1mm/s, pulse energy is kept at 1.5 μJ , and the focal spot diameter is 2.2 μm. For 120 kHz, the length and width of modification are 62.9 μm and 11.9 μm, respectively. For 20 kHz, the length and width of modification are 54.2 μm and 8.7 μm, respectively. Comparing results at 20 kHz and 120 kHz, the repetition rate has a 6-fold difference, while the difference in modification size is significantly less pronounced than varying the pulse energy (Fig. 5). So pulse energy affects morphology of modifications more than repetition rate.

3.3.4 The influence of input beam shape on modification

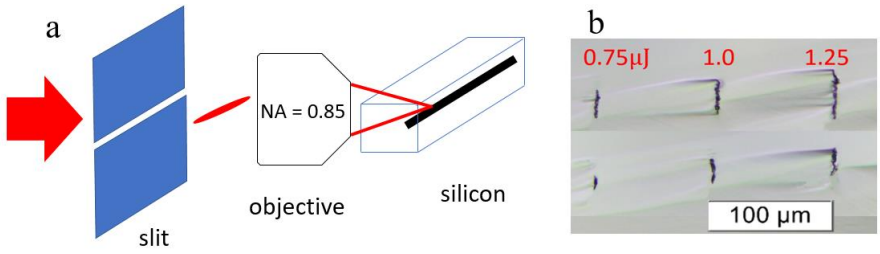

Fig.8. **a**, Schematic diagram of the experimental setup with a slit. **b**, Modifications with and without slit. Upper row is without slit, and lower row is with slit. From left to right, the pulse energy is 0.75, 1.0, and 1.25 μJ, respectively. The repetition rate is 20 kHz, and the scanning speed is 10 mm/s. The laser light is from top to bottom.

The dependence of modification morphology on input beam shape is also investigated. Since the sample is translated transverse to the writing beam to form the modification, the cross section is related to the shape of the focal volume. Typically, the focal intensity distribution of a beam focused into a silicon wafer is several times larger in the axial direction than the transverse directions, potentially resulting in highly asymmetric waveguides. To obtain a circular cross

sectional profile, one can employ multiple scans of the writing beam across the sample, shifting the beam transversely between each pass [23]. Several methods have been used in the past to shape the writing beam's focal volume [24]. The simplest of these is to use a physical slit before the objective, effectively reducing the NA in one dimension [25]. In our experiment, we create a slit by two paralleled razor blades. In Fig. 8a, the slit width is set at 1000 μm. We compare the morphology of modification with and without slit under three different pulse energies (0.75, 1.0 and 1.25 μJ), as shown in Fig. 8b. It can be seen that the morphology of modification without a slit is much more elongated than with a slit. An aspect ratio close to 1 is expected to be reached if we change the slit width and pulse energy. However, it might be not easy because the refractive index of 3.5 of silicon is so high that the slit width has to be very small, provoking too much energy losses.

3.3.5 Modifications under the SEM

To observe the laser treated areas using SEM, we made some modifications under a few selected conditions. We can see more details from the SEM images in Fig. 9 compared to the optical images included in this study. The modifications after cleaving are clear, but with some additional damage (e.g. cracks) caused by cleaving. After polishing and etching, the cracks disappear. Comparing a2, b2 and c2, we can see that the modifications are much longer when the scanning speed is 1mm/s than the one for the speed of 50mm/s. Also, some deep cracks appear at the modified site for the speed of 50 mm/s, indicating that material modification at this speed is more prone to etchant attack. Another possible reason for the enhanced contrast in Fig. 9(b2) is the change of silicon microstructures that reduces electron reflection in the SEM. Interestingly, the highest image contrast is obtained at a low energy dosage, suggesting the existence of an optimal combination of pulse energy, repetition rate and scanning speed that can enhance the internal modification. Line-shaped structures aligned horizontally in Fig. 9(a2) and (c2) are likely caused by the polishing process. Further characterization of laser modified areas will be conducted in the future to examine their 3D profile and study any changes in physical solid phase and optical and electrical properties.

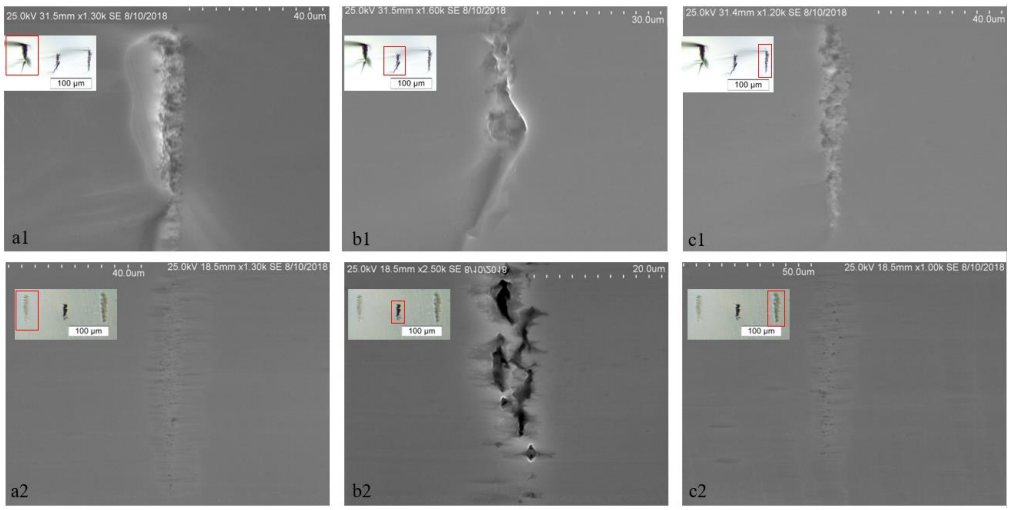

Fig.9. SEM images (Upper row is after cleaving, and lower row is after polishing and etching). a1, a2: The pulse energy is 1.5 μJ, the repetition rate is 100 kHz and the scanning speed is 1 mm/s. b1, b2: The pulse energy is 2 μJ, the repetition rate is 20 kHz and the scanning speed is 50 mm/s. c1, c2: The pulse energy is 2 μJ, the repetition rate is 20 kHz and the scanning speed is 1 mm/s. The inset images are taken from an optical microscope.

4 Conclusion

In conclusion, we use a fiber laser with 1.55 μm wavelength and 3.5 ns pulse duration to generate permanent modification inside intrinsic silicon wafers. Spherical aberration is found to be important and needs to be corrected for tight focusing at desired depth. While laser-induced modification can be clearly observed after cleaving the samples and exposing the cross sections, this modification disappears after mechanical polishing, suggesting the absence of severe damage such as cracks and voids. The morphology of subsurface modification is found to depend on the laser pulse energy, scanning speed, repetition rate and input beam shape. More specifically, the length and width of the modification increase with the increasing pulse energy and repetition rate, but decrease with the increasing scanning speed. The aspect ratio of the modification is affected by the shape of input beam.

Acknowledgments: Financial support for this work by the National Science Foundation under Grant No. CMMI-1537846 is gratefully acknowledged.

References

1 J. Ikeno, Y. Tani and A. Fukutani (1992) Development of Chipping-Free Dicing Technology Applying Electrophoretic Deposition of Ultrafine Abrasives, Annals of CIRP 41/1 351-354.

2 I.-H. Cho, S.-C. Jeong, J.-M Park and H.-D. Jeong (2001) The Application of Micro-Groove Machining for the Model of PDP Barrier Ribs, Journal of Materials Processing Technology 113 355-359

[3] S.B. Lee, Y. Tani, H. Ssato and T. Enomoto (2005) Development of a Dicing Blade with PhotopolymerizaResins for ImprovingMachinability, Annals of CIRP 54/1 293-296.

[4] G.C. Lim, A.T. Mai, D. Low and Q. Chen (2002) High Quality Laser Microcutting of Difficult-to-Cut Materials - Copper and Si Wafer, Proceedings of 21st International Congress on Applications of laser and Electro-Optics.

[5] F. Fukuyo, K. Fukumitsu and N. Uchiyama (2005) The Stealth Dicing Technologies and Their Application, Proceedings of 6th Laser Precision Microfabrication.

[6] W. Peng, X.F. Xu and L.F. Zhang (2002) Improvement of a Dicing Blade Using a Whisker Direction-Controlled by an Electric field, Journal of Materials Processing Technology 129, 377-379.

[7] R. Ebutt, S. Danyluk and I. Weisshaus (1996) Method to Evaluate Damage Induced by Dicing and Laser Cutting of Si Wafers, Microstructural Science 23, 89-94.

[8] K. Watanabe, Y. Ishizaka, E. Ohmura and I. Miyamoto (2000) Analysis of Laser Ablation Process in Semiconductor Due to Ultrashort Pulsed Laser with Molecular Dynamics Simulation, Proceedings of SPIE 3933, 46-55.

[9] P. Chall (2005) ALSI's Low Power Multiple Beam Technology for High Throughput and Low Damage Wafer Dicing, Proceedings of 65th Laser Materials Processing Conference, 211-215.

[10] D. Perrottet, A. Spiegel, F. Wagner, R. Housh, B. Richerzhagen and J. Manley (2004) Particle-free Semiconductor Dicing Using the Water Jet Guided Laser Technology, Proceedings of 21st International Congress on Applications of Lasers and Electro-Optics.

[11] Corboline, T. M., Rea, E. C., & Dunsky, C. M. (2003). High-power UV laser machining of silicon wafers. In Fourth International Symposium on Laser Precision Microfabrication (Vol. 5063, pp. 495-501). International Society for Optics and Photonics.

[12] Chambonneau, M., Li, Q., Chanal, M., Sanner, N., & Grojo, D. (2016). Writing waveguides inside monolithic crystalline silicon with nanosecond laser pulses. Optics letters, 41(21), 4875-4878.

[13] Yu, X., Wang, X., Chanal, M., Trallero-Herrero, C. A., Grojo, D., & Lei, S. (2016). Internal modification of intrinsic and doped silicon using infrared nanosecond laser. Applied Physics A, 122(12), 1001.

[14] Verburg, P. C., Römer, G. R. B. E., & Huis, A. J. (2014). Two-photon–induced internal modification of silicon by erbium-doped fiber laser. Optics express, 22(18), 21958-21971.

[15] Mori, M., Shimotsuma, Y., Sei, T., Sakakura, M., Miura, K., & Udono, H. (2015). Tailoring thermoelectric properties of nanostructured crystal silicon fabricated by infrared femtosecond laser direct writing. physica status solidi (a), 212(4), 715-721.

[16] Ito, Y., Sakashita, H., Suzuki, R., Uewada, M., Luong, K. P., & Tanabe, R. (2014). Modification and machining on back surface of a silicon substrate by femtosecond laser pulses at 1552 nm. Journal of Laser Micro Nanoengineering, 9(2), 98.

[17] Grojo, D., Mouskeftaras, A., Delaporte, P., & Lei, S. (2015). Limitations to laser machining of silicon using femtosecond micro-Bessel beams in the infrared. Journal of Applied Physics, 117(15), 153105.

[18] Nasse, M. J., & Woehl, J. C. (2010). Realistic modeling of the illumination point spread function in confocal scanning optical microscopy. Josa a, 27(2), 295-302.

[19] Yu, X., Liao, Y., He, F., Zeng, B., Cheng, Y., Xu, Z., ... & Midorikawa, K. (2011). Tuning etch selectivity of fused silica irradiated by femtosecond laser pulses by controlling polarization of the writing pulses. Journal of Applied Physics, 109(5), 053114.

[20] Zavedeev, E. V., Kononenko, V. V., & Konov, V. I. (2015). Delocalization of femtosecond laser radiation in crystalline Si in the mid-IR range. Laser Physics, 26(1), 016101.

[21] Leyder, S., Grojo, D., Delaporte, P., Marine, W., Sentis, M., & Utéza, O. (2013). Non-linear absorption of focused femtosecond laser pulses at 1.3 μm inside silicon: independence on doping concentration. Applied Surface Science, 278, 13-18.

[22] Osellame, R., Hoekstra, H. J., Cerullo, G., & Pollnau, M. (2011). Femtosecond laser microstructuring: an enabling tool for optofluidic lab-on-chips. Laser & Photonics Reviews, 5(3), 442-463.

[23] Le Harzic, R., Breitling, D., Weikert, M., Sommer, S., Föhl, C., Valette, S., ... & Dausinger, F. (2005). Pulse width and energy influence on laser micromachining of metals in a range of 100 fs to 5 ps. Applied Surface Science, 249(1-4), 322-331.

[24] Nasu, Y., Kohtoku, M., & Hibino, Y. (2005). Low-loss waveguides written with a femtosecond laser for flexible interconnection in a planar light-wave circuit. Optics letters, 30(7), 723-725.

[25] Ams, M., Marshall, G. D., Spence, D. J., & Withford, M. J. (2005). Slit beam shaping method for femtosecond laser direct-write fabrication of symmetric waveguides in bulk glasses. Optics express, 13(15), 5676-5681.

Chapter 3 - Nanosecond laser writing of straight and curved waveguides in silicon with shaped beams

This work was published in the paper "Nanosecond laser writing of straight and curved waveguides in silicon with shaped beams," X Wang, X Yu, M Berg, B DePaola, H Shi, P Chen, L Xue, X Chang and S Lei, Journal of Laser Applications 32 (2), 022002

Abstract

We demonstrate a method for transverse writing of optical waveguides in a crystalline silicon wafer using a nanosecond laser with a shaped beam profile that is formed by a pair of cylindrical lenses. In contrast to traditional writing methods, this method avoids forming asymmetric waveguide profiles. Both straight and curved waveguides are written with a nearly circular transverse guide-profile and are found to support single-mode propagation for $1550\ \mathrm{nm}$ wavelength light. The propagation loss for this wavelength is also measured.

1. **Introduction**

The use of lasers to write waveguides in dielectrics, especially glass, is well-established, e.g., see [1-6]. Generally, the method is based on laser-induced structural modifications that manifest a refractive-index contrast with the surrounding unmodified regions in the dielectric [7-15]. Despite the importance of silicon (Si) in the microelectronics industry and its growing importance in photonics, studies on waveguide writing in this material are limited. Previous work reports two-photon–induced internal modification of Si using an erbium-doped fiber laser pulsed at 3.5 ns [16]. With a similar method, elongated structures are reported in [17]. Investigations of the properties of the internal modifications generated by ns laser pulses are presented in [18-20]. Direct writing of single-mode waveguides in Si with ps laser pulses is demonstrated in [21]. Depressed-cladding waveguides inside bulk silicon written by ns laser pulses are achieved in [22]. Waveguides can also be written using femtosecond (fs) pulses as demonstrated in [12], even though the induced modifications are generated only at the SiO_2/Si interface. Waveguides deep into bulk Si are first reported with 350 fs laser pulses at a wavelength of 1550 nm in [23, 24] where a 10^{-4} refractive-

index change in magnitude is seen. Local modification in bulk Si with sub-100-fs laser pulses is achieved in [25] with single pulses tightly focused at the center of silicon spheres using extreme solid-immersion focusing.

In general, two methods can be used to write waveguides in Si: longitudinal and transverse [6]. In longitudinal writing, the sample is translated along the writing-beam propagation direction. The advantage of this method is that the guides have symmetric profiles and their transverse size is determined by the focal-spot size of the objective lens used to concentrate the laser light. That means, however, that the waveguide length is limited by the objective-lens focal length and spherical aberration that may distort the focal shape. The waveguides presented in [17, 22 - 24], which use longitudinal writing, are typically less than several millimeters in length. In transverse writing, the sample is translated perpendicular to the writing-beam propagation direction [6]. Thus, the waveguide length is not restricted by the working distance of the objective lens but the waveguide profile takes an asymmetric droplet-like shape. This shape is due to the Gaussian profile of the writing beam at its focal waist, with a diameter of $D = 2w_0$ and confocal parameter of $b = 2\pi w_0^2/\lambda$, where w_0 is the $1/e^2$ waist radius and λ is the wavelength.

For focal-spot diameters of a few micrometers, there is a large difference between D and b. The asymmetry becomes particularly severe when the waveguide size D is increased, which would reduce the efficiency of fiber butt coupling in conventional telecommunications setups [3]. In this Letter, we use the transverse method and a beam-shaping technique from [26] that uses a pair of cylindrical lenses to astigmatically shape a ns-pulsed laser beam to write waveguides with a more circular cross section. We demonstrate both straight and curved waveguides. To our knowledge, this is the first time that high quality waveguides are written deep inside monocrystalline Si using the transverse method with such astigmatic beam shaping.

For an astigmatically focused Gaussian beam with the major axis in the x direction, minor axis in the y direction, and propagation along the z direction, the beam radius along the x or y directions is R_x and R_y, respectively. The spot diameter in the x-z plane is

$$D_x = 2w_0 = 1.22\frac{\lambda}{NA} \qquad (1)$$

while the confocal parameter is

$$b = 2\pi w_0^2/\lambda. \quad (2)$$

The spot diameter in the y-z plane is taken as

$$D_y = D_x \frac{R_x}{R_y} \quad (3)$$

and b is the same as in the x-z plane. By tuning the ratio of R_x and R_y, we can achieve

$$D_y = b \quad (4)$$

resulting in a circular spot-profile in the y-z plane. From Eqs. (2) and (4), we have

$$\frac{R_x}{R_y} = \frac{0.61\pi}{NA}. \quad (5)$$

Including the refractive index n of the Si sample, Eq. (5) becomes

$$\frac{R_x}{R_y} = \frac{0.61\pi n}{NA}. \quad (6)$$

Figure 1(a) and (b) shows, respectively, the calculated cross-sectional distributions of laser intensity at the focal point in the y-z and x-z planes where R_x and R_y satisfy Eq. (6). The distributions are generated from the formulae based on [26] modified to account for the refractive index of Si. Because of the difficulty in direct measurement of beam profile in the yz and xz planes, measurements in the xy plane at different z positions are made for verification with the calculated profiles. The favorable comparison between the measured and theorecitally predicted profiles (not shown here) indicates that the real beam profile near the focal point should match these in Fig. 1(a) and (b). As seen from Fig. 1(a) and (b) the intensity distribution is more circular in the y-z than in the x-z plane. In the following experiment, the beam is scanned along the x-axis so that the waveguide cross-section is determined by this nearly circular profile, as shown by the modification in Fig. 1(c). Note that a similar beam profile can be generated with a slit [6]. We choose a cylindrical lens pair here because more laser energy can be delivered to the Si than with a slit.

2. Experimental details

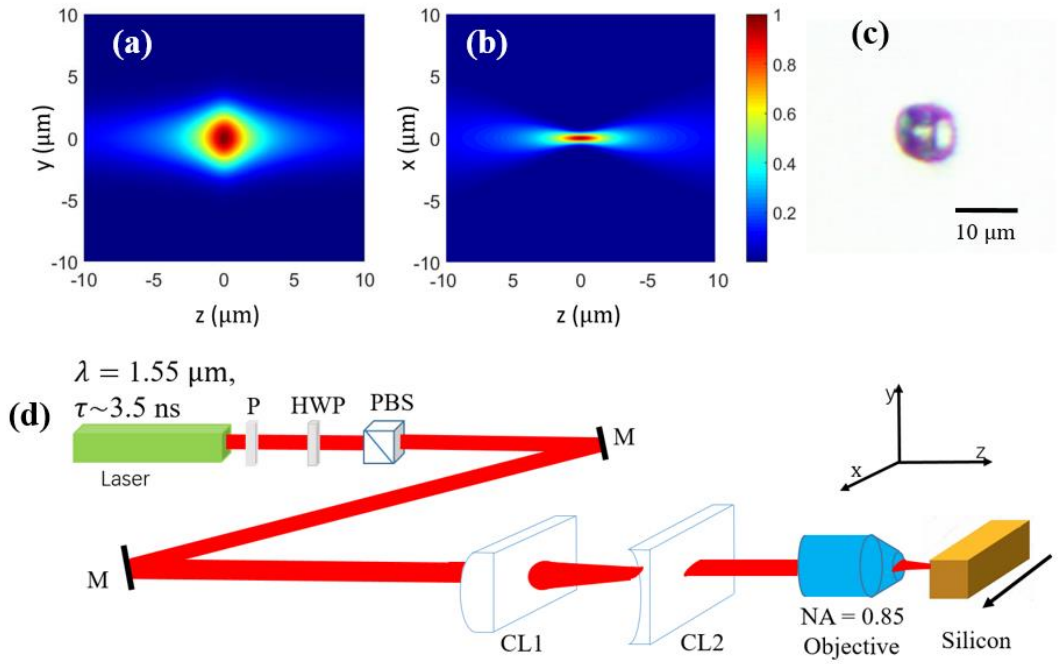

Fig. 1. Waveguide writing in Si. Shown in (a) and (b), respectively, are the calculated laser beam profiles near the focus of the objective in the y-z and x-z planes displaying a near circular and an elliptical Gaussian structure. In (d) is the experimental arrangement we use for waveguide writing consisting of a polarizer (P), half-wave plate(HWP), polarizing beam splitter (PBS), mirror (M), cylindrical lens pair (CL1, CL2), and microscope objective. In (c) is an image of the cross section of a waveguide in Si (after a chemical etching process) in the y-z plane made with this method. The scanning speed for this example is 50 mm/s with a pulse energy of 1.25 μJ and laser repetition rate of 20 kHz.

The experimental setup is depicted in Fig. 1. (d) and the samples used throughout the study are (100)-oriented, 1-mm thick intrinsic Si wafers with a resistivity of >200 Ω·cm. We use an IR laser to write the waveguides due to the low light-absorption of Si in the IR region. Specifically, the laser source (MWTech, PFL-1550) has a wavelength of λ =1550 nm and produces pulses of length τ = 3.5 ns (full width at half-maximum) and can be operated at various repetition rates with a maximum pulse energy of 20 μJ. The output beam has a $1/e^2$ diameter of 6 mm. A half waveplate in conjunction with a polarizing beam splitter is used to control the pulse energy by rotation of the

waveplate. Following reflection from two mirrors to allow for fine beam-alignment, the beam is shaped by a pair of cylindrical lenses. These are separated by a distance of $|f_1| - |f_2|$, where f_1 = 30 cm (f_2 = -3 cm) is the focal length of CL1 (CL2). The beam is then focused into a Si sample by a microscope objective (NA = 0.85, Olympus, Model LCPLN100XIR) that is corrected for spherical aberration. At focus in the x-z plane, the beam has a theoretical diameter at $1/e^2$ of $2w_0 = 1.22\,\lambda/NA = 2.2$ μm, with Rayleigh lengths of z_R = 2.6 μm in air and $z_R \approx 9.2$ μm in Si. In the y-z plane, the spot radii along the y and z directions are both 9.2 μm.

Silicon samples of 20×20 mm^2 in size are mounted on a motorized XYZ stage (Newport, Model ILS100PP). The focal depth in the Si sample is controlled by moving the sample along the laser beam propagation direction (z direction), and the waveguide is written by scanning the sample along the x direction at a constant speed, see Fig. 1(d). To achieve a desired writing depth in the Si sample, the focus is first positioned on the illuminated surface by observing plasma emission. Then, the desired writing depth (d=0.5 mm) is obtained by moving the sample toward the objective by d/n, where n = 3.5 is the refractive index of silicon at λ =1550 nm. Then, the Si sample is scanned along the x direction to form an extended waveguide structure with the length of 5mm. The sample scanning speed is 50 mm/s and the laser-pulse energy is varied from 1.0 to 2.0 μJ.

3. Results and discussion

To examine the cross section of the resulting waveguides, the sample is cleaved perpendicular to the scanning direction, i.e., along the y direction such that the cleaved surface is in the (110)-plane. This surface is then polished and immersed in a 50 wt. % KOH solution and etched for 5 minutes in an ultrasonic bath. Then, the cleaved surface is observed with a conventional optical microscope. We find that the cross section of the modified region inside the Si is close to circular in shape when the pulse energy is 1.25 μJ, and the scanning speed is 50 mm/s, as shown in Fig. 1(c). The colors in the cross section may originate from light diffraction due to microstructures under white-light

illumination. We observe modification only within the Si sample and none on either the front (illuminated) or the back (exit) surface of the samples.

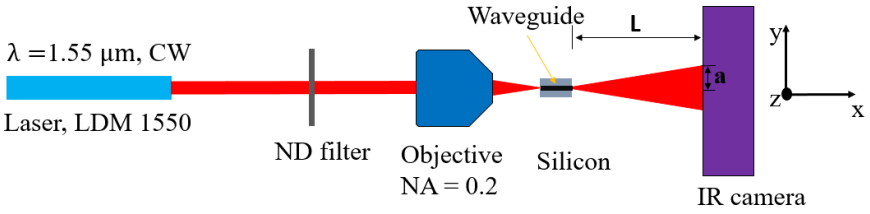

Fig. 2. Experimental arrangement used to characterize the waveguide performance. The same laser is used as in Fig. 1 except it is operated in CW mode. A neutral density filter is used to attenuate the beam intensity and the light transmitted through the waveguide is recorded with an InGaAs sensor. Note that from comparison with Fig. 1(d), the waveguide extends along the x direction.

To further characterize the waveguide, we measure its numerical aperture (NA) by coupling into it a CW beam from the λ =1550 nm laser using another microscope objective with $NA = 0.2$, see Fig. 2. The light emerging from the waveguide is then recorded with an InGaAs camera at a distance of L from the waveguide exit. The far-field (L = 2.6 cm) and near-field (L = 3 mm) intensity distributions of light from the waveguide can be measured and an example of this is shown in Fig. 3(a) and (b). The far-field distribution is then fit to a Gaussian profile as shown Fig. 3(d), yielding a mode waist radius of a=1 mm for the 10 µm diameter waveguide in Fig. 1(c). The NA of the waveguide is then determined by $NA = a/L = 0.038$ [22]. Lastly, by approximating the laser-induced modification to be step-like in refractive index following [27], we estimate the refractive-index change Δn from NA=$\sqrt{2n\Delta n}$ to be $\Delta n = 2.0 \times 10^{-4}$. Note that this value for Δn is comparable to that found by others [22]. The v- number of the waveguide is ~ 1.54, which implies that the waveguide operates in a single mode for this wavelength.

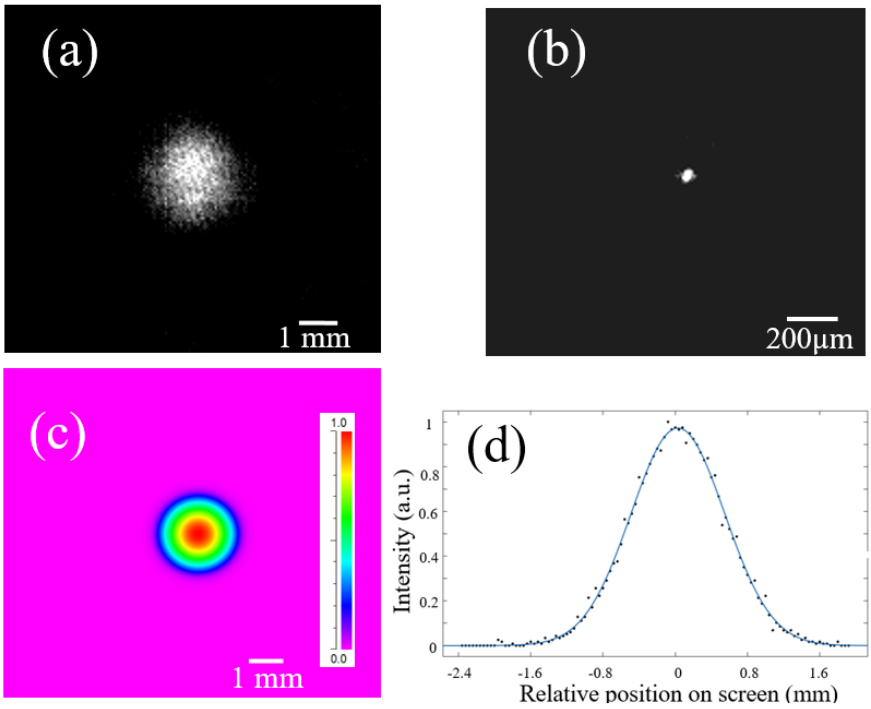

Fig. 3. Characterization of the waveguide performance. In (a) and (b) are the far-field and near-filed light intensity distribution emerging from the waveguide in relation to the measurement arrangement of Fig. 2, respectively. In (c) is the simulated far-field light intensity distribution. The distribution of (a) is fit (solid line) to a Gaussian profile in (d).

To determine the loss of the waveguide, we measure the power of the laser light before and after passing through the waveguide. We calculate the damping loss by the relationship $\alpha = 10\log(P_1/P_2)/d$, where d is the waveguide length, P_1 is the input power, and P_2 is the output power from the waveguide. Subtracting the Fresnel reflection (3.2 dB) and the coupling loss (14.4dB), the typical value is 2.8 dB/cm. The scattered loss is included in the damping loss. Based on our calculation, since our sample is a wafer, not a cylindrical rod, the loss caused by the non-guided light is found to be negligible. In addition, a numerical simulation of the beam propagation based on the calculated refractive index profile is performed using the software "BeamPROP" [28]. The result in Fig. 3(c) is in good agreement with the measured far-field profile in Fig. 3(a).

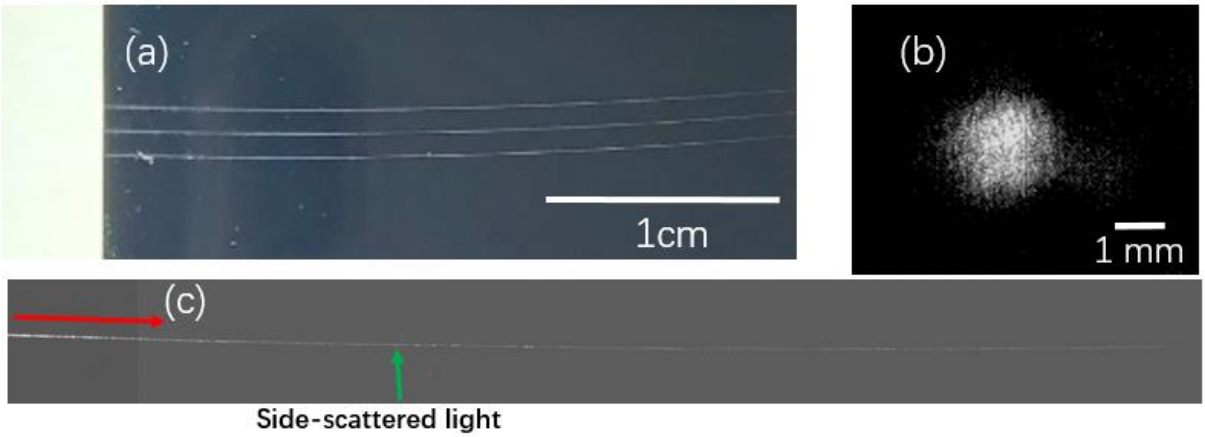

Fig. 4. Writing of curved waveguides. Surface marks on the Si sample indicating the location of the curved waveguides beneath are shown in (a). The radius of curvature of these waveguides is 22 cm. Shown in (b) is the far-field intensity of guided light exiting the curved waveguide. Observation of the side-scattered light along the waveguide is presented in (c). The red arrow indicates the light propagation direction.

To further demonstrate the light guiding capability of our transverse method, we write a curved waveguide. The sample is mounted on a rotation stage (Newport, SR50PP) and operated at a speed of $0.175\ \mathrm{rad/s}$. The radius of curvature of the resulting waveguide is 22 cm with a scanning speed of 38.5 mm/s resulting in an arc length of the waveguide segment of 30 mm. Also, the waveguide is written at the same depth as the straight waveguides. To help locate the position of these curved waveguides, marks are scribed on the Si sample surface, as shown in Fig. 4(a). Then the loss of the waveguide is calculated by measuring the input power and out power, the same method as used for the straight waveguides. The result is 3.3 dB/cm, which is similar to the value measured for the straight waveguide. Figure 4(b) shows the far-field intensity distribution of the guided light emerging from a curved waveguide. Notice that the quality of the profile, i.e., Gaussian like, is similar to that of the straight waveguide in Fig. 3(a). Also notice that the side-scattered light in Fig. 4(c) clearly shows that the light is confined to propagate along the curve. That observation supports the conclusion that both the straight and curved guides support single-mode propagation.

It should be noted at this point that the typical loss of waveguides written in bulk silicon with different pulse durations is about a few dB/cm as reported in the literature, which is more than one

order of magnitude higher than that of glass waveguides [29]. A major source of waveguide loss can be attributed to light scattering from defects generated in the laser writing process. In addition, dopant in silicon may affect the structural formation of the laser written waveguides. It is shown in one of our previous studies [18] that at a high doping level, linear absorption of light by the initial free carriers before the focus reduces the pulse energy reached at the focus and thus the size of the induced modification.

In general, to realize the full potential of this technique and manufacture waveguides with a large refractive-index contrast and improved performance, further work is needed. In particular, it is necessary to have a more complete understanding of the physical processes involved from nonlinear absorption to the nature of material modification/damage. For example, do the material modifications result from the Si being changed from single crystalline to polycrystalline or perhaps amorphous states?

4. Conclusion

In summary, we demonstrate that a transverse-writing method involving a shaped beam can produce straight and curved waveguides. The elliptical Gaussian mode created by a pair of cylindrical lenses enables control of the beam waist dimension in the direction perpendicular to the beam scanning direction through the sample. Thus, waveguides with a symmetric profile can be written. In order to demonstrate the potential of the method, a curved waveguide in Si is written, featuring a loss of 3.3 dB/cm. This method suggests the possibility that complex waveguide networks could be laser-written in Si, e.g., by combining the translation and rotation writing modes described here, which could have applications in silicon photonics, MEMS devices, optoelectronics, microfluidics, lab-on-chip devices, etc.

Funding. Financial support for this work by the National Science Foundation under grants CMMI-1537846 and 1665456 and the U.S. Air Force Office of Scientific Research grant FA9550-19-1-0078 are gratefully acknowledged.

Disclosures. The authors declare no conflicts of interest.

References

[1] K. M. Davis, K. Miura, N. Sugimoto, and K. Hirao, "Writing waveguides in glass with a

femtosecond laser," Opt. Lett. **21**, 1729 (1996).

[2] J. W. Chan, T. Huser, S. Risbud, and D. M. Krol, "Structural changes in fused silica after exposure to focused femtosecond laser pulses," Opt. Lett. **26**, 1726 (2001).

[3] R. Osellame, S. Taccheo, M. Marangoni, R. Ramponi, P. Laporta, D. Polli, S. De Silvestri, and G. Cerullo, "Femtosecond writing of active optical waveguides with astigmatically shaped beams," J. Opt. Soc. Am. B **20**, 1559 (2003).

[4] A. Zoubir, M. Richardson, L. Canioni, A. Brocas, and L. Sarger, "Optical properties of infrared femtosecond laser-modified fused silica and application to waveguide fabrication," JOSA B **22**(10), 2138–2143 (2005).

[5] K. Itoh, W. Watanabe, S. Nolte, and C. B. Schaffer, "Ultrafast Processes for Bulk Modification of Transparent Materials," MRS Bull. **31**(08), 620–625 (2006).

[6] M. Beresna, M. Gecevicius, and P. G. Kazansky, "Ultrafast laser direct writing and nanostructuring in transparent materials," Adv. Opt. Photonics **6**(3), 293–339 (2014).

[7] F. Chen and J. R. V. de Aldana, "Optical waveguides in crystalline dielectric materials produced by femtosecond-laser micromachining," Laser Photonics Rev. **8**, 251–275 (2014).

[8] S.-H. Cho, H. Kumagai, and K. Midorikawa, ''In situ observation of dynamics of plasma formation and refractive index modification in silica glasses excited by a femtosecond laser,'' Opt. Commun. 207, 243–253 (2002)

[9] Y. Sikorski, A. A. Said, P. Bado, R. Maynard, C. Florea, and K. A. Winick, "Optical waveguide amplifier in Nd-doped glass written with near-IR femtosecond laser pulses," Electron. Lett. **36**, 226 (2000).

[10] A. M. Streltsov and N. F. Borrelli, "Fabrication and analysis of a directional coupler written in glass by nanojoule femtosecond laser pulses," Opt. Lett. **26**, 42 (2001).

[11] C. B. Schaffer, A. Brodeur, J. F. García, and E. Mazur, "Micromachining bulk glass by use of femtosecond laser pulses with nanojoule energy," Opt. Lett. **26**, 93 (2001).

[12] A. H. Nejadmalayeri, P. R. Herman, J. Burghoff, M. Will, S. Nolte, and A. Tünnermann, "Inscription of optical waveguides in crystalline silicon by mid-infrared femtosecond laser

pulses," Opt. Lett. **30**, 964 (2005).

[13] C. W. Carr, H. B. Radousky, A. M. Rubenchik, M. D. Feit, and S. G. Demos, "Localized Dynamics during Laser-Induced Damage in Optical Materials," Phys. Rev. Lett. **92**, (2004).

[14] M. Bazzan, C. Sada, "Optical waveguides in lithium niobate: Recent developments and applications," **2**, 040603 (2015)

[15] A. Stone, H. Jain, V. Dierolf, M. Sakakura, Y. Shimotsuma, K. Miura, K. Hirao, J. Lapointe, and R. Kashyap, "Direct laser-writing of ferroelectric single-crystal waveguide architectures in glass for 3D integrated optics," Sci. Rep. **5**, 1–10 (2015).

[16] P. C. Verburg, G. R. B. E. Römer, and A. J. Huis In 't Veld, "Two-photon-induced internal modification of silicon by erbium-doped fiber laser.," Opt. Express **22**, 21958–71 (2014).

[17] M. Chambonneau, Q. Li, M. Chanal, N. Sanner, and D. Grojo, "Writing waveguides inside monolithic crystalline silicon with nanosecond laser pulses," Opt. Lett. **41**, 4875 (2016).

[18] X. Yu, X. Wang, M. Chanal, C. A. Trallero-Herrero, D. Grojo, and S. Lei, "Internal modification of intrinsic and doped silicon using infrared nanosecond laser," Appl. Phys. A Mater. Sci. Process. **122**, 1–7 (2016).

[19] X. Wang, X, Yu, H. Shi, X. Xian, M. Chambonneau, D. Grojo, B. DePaola, M. Berg and S. Lei, "Characterization and control of laser induced modification inside silicon" J. Laser Appl. **31**, 022601 (2019)

[20] M. Chambonneau, X. Wang, X. Yu, Q. Li, D. Chaudanson, S. Lei, and D. Grojo, "Positive- and negative-tone structuring of crystalline silicon by laser-assisted chemical etching," Opt. Lett. **44**, 1619 (2019).

[21] H. Kämmer, G. Matthäus, S. Nolte, M. Chanal, O. Utéza, and D. Grojo, "In-volume structuring of silicon using picosecond laser pulses," Appl. Phys. A Mater. Sci. Process. **124**, 1–6 (2018).

[22] A. Turnali, M. Han, and O. Tokel, "Laser-written depressed-cladding waveguides deep inside bulk silicon," J. Opt. Soc. Am. B **36**, 966 (2019).

[23] O. Tokel, A. Turnall, G. Makey, P. Elahi, T. Çolakoğlu, E. Ergeçen, Ö. Yavuz, R. Hübner,

M. Zolfaghari Borra, I. Pavlov, A. Bek, R. Turan, D. K. Kesim, S. Tozburun, S. Ilday, and F. Ö. Ilday, "In-chip microstructures and photonic devices fabricated by nonlinear laser lithography deep inside silicon," Nat. Photonics **11**, 639–645 (2017).

[24] I. Pavlov, O. Tokel, S. Pavlova, V. Kadan, G. Makey, A. Turnali, Ö. Yavuz, and F. Ö. Ilday, "Femtosecond laser written waveguides deep inside silicon," Opt. Lett. 42(15), 3028–3031 (2017).

[25] M. Chanal, V. Y. Fedorov, M. Chambonneau, R. Clady, S. Tzortzakis, and D. Grojo, "Crossing the threshold of ultrafast laser writing in bulk silicon," Nat. Commun. **8**, 1–6 (2017).

[26] Y. Cheng, K. Sugioka, K. Midorikawa, M. Masuda, K. Toyoda, M. Kawachi, and K. Shihoyama, "Control of the cross-sectional shape of a hollow microchannel embedded in photostructurable glass by use of a femtosecond laser," Opt. Lett. **28**, 55 (2003).

[27] M. Ams, G. D. Marshall, D. J. Spence, and M. J. Withford, "Slit beam shaping method for femtosecond laser direct-write fabrication of symmetric waveguides in bulk glasses," Opt. Express **13**, 5676 (2005).

[28] https://www.synopsys.com/optical-solutions/rsoft/passive-device-beamprop.html

[29] Y. Nasu, M. Kohtoku, Y. Hibino, "Low-loss waveguides written with a femtosecond laser for flexible interconnection in a planar light-wave circuit," Opt Lett. 2005 Apr 1;30(7):723-5.

Chapter 4 - Curved Waveguides in Silicon Written by a Shaped Laser Beam

This work was published in the paper “Curved Waveguides in Silicon Written by a Shaped Laser Beam,” X Wang, X Yu, MJ Berg, P Chen, B Lacroix, S Fathpour and S Lei , Optics Express 29 (10), 14201-14207

Abstract

We demonstrate, for the first time, the direct writing of curved optical waveguides in monocrystalline silicon with curve radii from two mm to six cm. The bending loss of the curved waveguides is measured and a good agreement with theoretical values is found. Raman spectroscopy measurements suggest the formation of inhomogeneous amorphous and polycrystalline phases in the laser-modified region. This direct laser-writing method may advance fabrication capabilities for integrated 3D silicon photonic devices.

1. Introduction

Laser writing of optical waveguides inside dielectrics, especially glass, has been well developed in the past decades [1,2]. Generally, the waveguide is generated by producing a refractive-index contrast between the laser-induced structural modifications and the surrounding unmodified regions [3-5]. Two-photon–induced internal modification of Si was studied by Verburg et al. [6]. Investigations of the elongated structures and internal modifications formed by ns laser pulses were reported in [7-10]. Single-mode waveguides written inside Si with ns, ps and fs laser pulses were also demonstrated in [11-15]. Temporal contrast of the ultrashort pulses is proved to be a critical driving parameter in the process of modification formation [16].

Longitudinal writing and transverse writing are two commonly used methods to write waveguides [1]. The waveguides lengths are often less than several millimeters in the longitudinal writing because of the limitation of the lens focal distance [7,10-15]. On the other hand, the transverse

method provides the possibility of writing long waveguides without the restriction of lens working distance. However, the cross-sectional shape of the waveguide is usually asymmetric in the transverse method. Fortunately, this drawback could be overcome by using shaped beams [2,17,18].

An advantage of the transverse writing method is that it provides more flexibility to write waveguide paths with complex shapes, i.e., shapes other than linear paths. Semicircular, or curved, waveguide paths are one example, which we demonstrate here. We study the performance of the curved waveguides, specifically with regard to the bending loss. The theory of bending loss in curved waveguides is established [19-24]. Marcuse [21] developed the first loss formula for optical fibers with a constant radius of curvature.

Our previous work has shown the possibility of transverse writing of waveguides inside silicon by shaped beams [20]. In this paper, we write curved waveguide paths with different radii and measure the bending loss caused by the curvature. We compare our measurements with calculated results based on the theory and find that they are in good agreement. Finally, we conduct Raman spectroscopy of the waveguides and show the formation of amorphous and polycrystalline silicon.

2. Experimental setup

The silicon wafers used in this study are intrinsic, (100)-oriented, and 1-mm thick. The resistivity is greater than 200 Ω·cm. The experimental arrangement used for writing is shown in Fig. 1. The wavelength and the pulse duration of the laser (MWTech, PFL-1550) are 1550 nm and 3.5 ns, respectively. The repetition rate is 20 kHz and the maximum pulse energy is 20 μJ. The diameter of the output beam is 6 mm. A pair of cylindrical lenses, CL1 and CL2, are used to shape the beam. The distance between the two lenses is $|f_1| - |f_2|$, where f_1(30 cm) and f_2 (-3 cm) are the focal lengths of the two lenses, respectively. A spherically corrected objective lens (Olympus, LCPLN100XIR, NA = 0.85) is used to focus the beam into the silicon sample. At the focal point in the x-z plane, the focal spot size is $2w_0 = 1.22\,\lambda/NA = 2.2$ μm, and the Rayleigh length is z_R = 2.6 μm in air and $z_R \approx 9.2$ μm in Si. Along the y and z directions, the spot radii are both 9.2 μm [20].

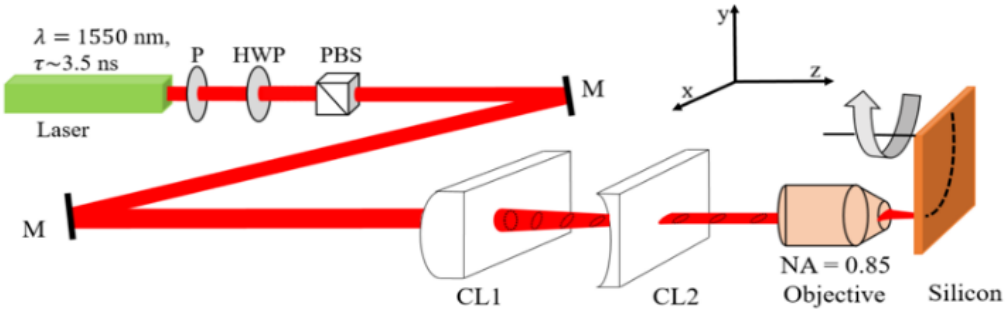

Fig. 1. Experimental arrangement used for transverse writing of semicircular, i.e., curved waveguides. The combination of a polarizer (P), half-wave plate (HWP), and polarizing beam splitter (PBS) is used to tune the output power. Other optical elements include mirrors (M), and two cylindrical lenses (CL1) and (CL2). A Si wafer sample is mounted on a rotation stage with the rotation axis parallel to the *z*-axis as shown.

The silicon samples in our experiment are 40×40 mm^2 in size and they are mounted on a motorized rotation stage (Newport, SR50PP), which itself is mounted on an XYZ translation stage (Newport, ILS100PP). The laser light is focused at the depth of 0.5 mm. Curved waveguides are written by rotating the silicon sample. The laser writing speed for all the curved waveguides with different radii is kept at 38.5 mm/s by controlling the angular speed of the rotation stage. The use of the rotation stage ensures that the waveguides are written by the same beam profile [20]. The rotation stage is rotated through 90° for each waveguide and a total of 14 of quarter-circle waveguides are written with radii of curvature ranging from 0.2 cm to 6 cm. Each waveguide is buried in the silicon at a depth of 0.5 mm. Marks are scribed on the sample surface to aid locating the waveguides in later analysis.

3. Results and Discussion

Figure 2 shows three of the 14 curved waveguides written with this method. The radii are 0.5 cm, 2.5 cm, and 5 cm. To obtain this figure, we couple a continuous wave (CW) laser beam by an objective (NA = 0.2) at λ = 1550 nm into each waveguide at the locations indicated by the red arrows at the bottom of Fig. 2. A portion of the light scatters out of the waveguide during

propagation due to material defects in the waveguide. We image this scattered light with an IR camera and objective lens (NA=0.3) across the portions of the wafer surface where the illuminated waveguide resides, i.e., portions of the *x*-*y* plane. Because the field of view of the objective lens is not sufficient to cover the (90°) arc length of an entire waveguide, multiple images are taken and then stitched together manually to form a mosaic revealing the entire waveguide. Figure 2 clearly shows that light is confined and propagates along these curved waveguides, exhibiting a gradual decay in intensity along the arc. It should be noted that the diverging light exceeding the acceptance angle of the waveguide diffracts out of the waveguide and thus does not contribute to the decay of the guided light. Notice that the light decays faster in waveguides with a smaller radius of curvature. As far as we know, this is the first time that multiple curved waveguides of different radii inside silicon are written by a shaped laser beam.

Next, we measure the bending loss of the curved waveguides of different radii [20]. The total loss α of a curved waveguide is expected to be the sum of the damping loss of a straight waveguide α_s with the same length as the curved waveguide plus the bending loss α_b caused by the curvature, i.e., $\alpha = \alpha_s + \alpha_b$. To determine α_s, we write a group of straight waveguides in Si with lengths equal to the arc length of the curved waveguides. Then, the power of the laser light through each of the straight and curved waveguide is measured. The damping loss is calculated by the equation $\alpha = 10 \log (P_1/P_2)/d$, where d, P_1 and P_2 are the waveguide length, input power and output power, respectively. We measure the input power P_1 at the entrance side of each waveguide and the output power P_2 at the exit side using a power meter. In this calculation, the loss due to the Fresnel reflection at both the front and back face (3.2 dB) and the coupling loss due to the NA mismatch between the objective lens and the waveguide (14.4 dB) are subtracted from the total loss. Note that scattering loss is included in the damping loss. By subtracting the measured damping loss of a straight waveguide α_s with length d from the α measured for a curved waveguide with arc length d, the bending loss α_b is determined. The dependence of α_b for curved waveguides on the radius of curvature R is shown in semi-log scale in Fig. 3 where the dots in the plot are the measurement results. For improved accuracy, we repeated these measurements five times for each of the 14 waveguides.

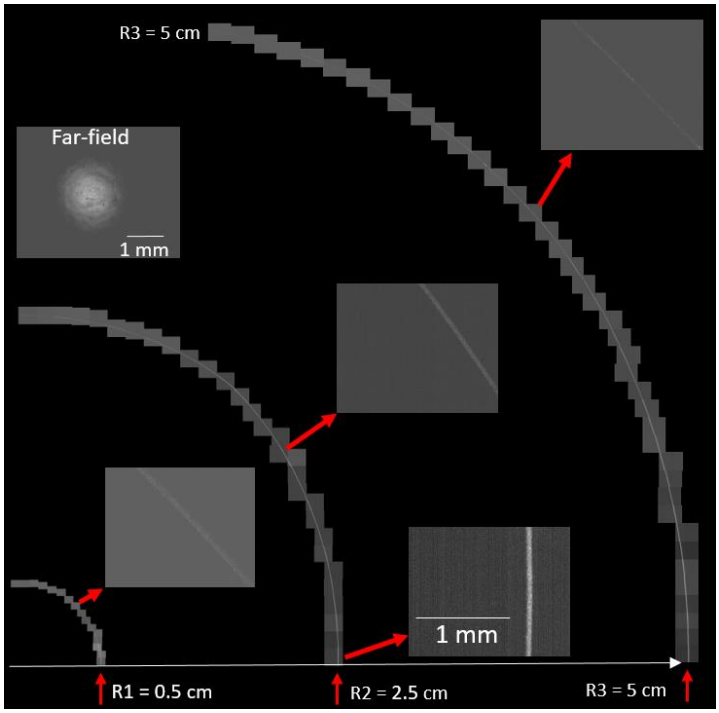

Fig. 2. Curved waveguides with different radii written in Si by the method in Fig. 1. Three waveguides in a single Si sample are shown with radii, R1=0.5 cm, R2=2.5 cm, and R3=5.0 cm as labeled. Infrared light is coupled into each guide from the bottom of the figure shown by the red vertical arrows. The light scatters as it travels along a waveguide arc and this scattered light is imaged with an IR camera over a limited field of view. By stitching together multiple images, a mosaic is formed revealing the entire waveguide arc length. Examples of single constituent images of a mosaic are shown via the remaining red arrows displayed. Note the decay of scattered light along a given waveguide as the light propagates up from its coupling point at the bottom of the figure. The top left image is the far-field (2.5 cm to the end facet of the waveguide) light intensity distribution from the curved waveguide with R = 2.5 cm.

To give context to our loss measurements, we compare to the theoretical treatment of bending loss in a curved waveguide given by [19]. The theory relates to a curved waveguide with a circular core cross-section of radius a and waveguide curvature radius R, where the bending loss is given by (simplified version of Eq. 3.6-7 in [19]) as:

$$\alpha_{\mathbf{b}}(\boldsymbol{R}) = \frac{ae^{2qa}}{\sqrt{\pi qR}}\left(\frac{h}{Vn_2}\right)^2 e^{-\frac{2Rq^3}{3\beta^2}}. \qquad (1)$$

Eq. (1) includes waveguide and mode parameters $q = \sqrt{\beta^2 - n_2^2 k_0^2}$, $h = \sqrt{n_1^2 k_0^2 - \beta^2}$, and $V = \sqrt{(ha)^2 + (qa)^2}$, where $k_0 = {}^{\omega}/_{c}$ and ω is the laser angular frequency, and c is the speed of light in vacuum. Here, n_1 and n_2 are the refractive index of core and cladding, respectively. Using the values $\lambda = 1.55$ μm $a = 5.0$ μm, $n_1 = 3.502$, $n_2 = 3.500$ appropriate for our sample, we obtain the propagation constant $\beta = 1.419 \times 10^7$ based on Eq. 3.3-26 in [19], i.e.

$$ha\frac{J_{l+1}(ha)}{J_l(ha)} = qa\frac{K_{l+1}(qa)}{K_l(qa)} \quad (2)$$

The red line in Fig. 3 represents Eq. (1) and one can see that the measurements for α_b are in a good agreement with the R dependence of the theory.

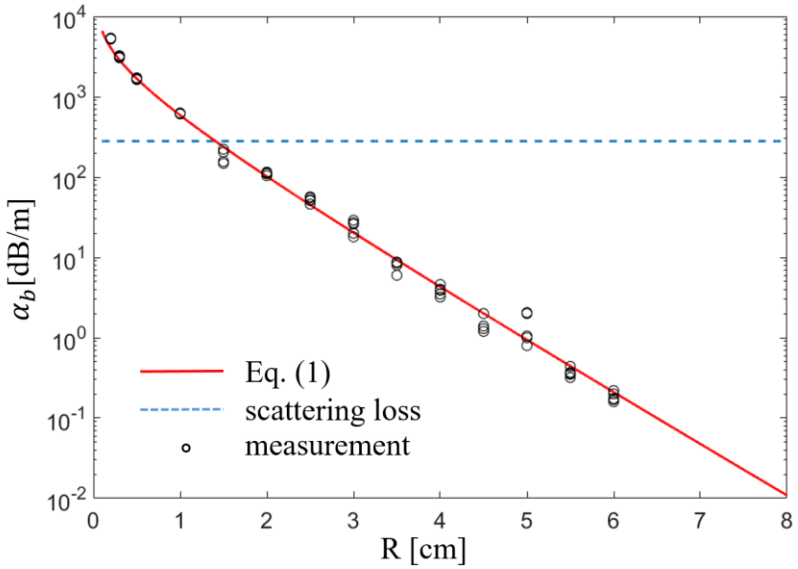

Fig. 3. Dependence of the bending loss α_b with curvature radius, R for the curved waveguides. The red curve is Eq. (1) while the blue line shows the scattering loss α_s (not bending loss) of a straight waveguide written with the same conditions as the curved waveguides.

In particular, notice in Fig. 3 that the measured bending loss α_b for the curved waveguides exhibit two clear trends that are also exhibited in Eq. (1). For R approximately larger than one cm, the plot shows a negative linear trend for α_b, which given the semi-log scale of the plot implies that α_b decays exponentially with increasing R. This is logical because as the radius of curvature approaches infinity, the bending loss should vanish as the waveguide becomes straight in that limit. Conversely, for R approximately less than one cm, we see a non-linear trend in Fig. 3. Again, due to the semi-log scale, this implies a hybrid exponential and power-law dependence,

the detail of which is revealed by reference to Eq. (1), i.e., the exponential R-dependence in the last term in Eq. (1) combined with the inverse $\sqrt{R}$ dependence in the first term. In other words, as the radius of curvature of the waveguide decreases, the bending loss grows precipitously, which in practical terms may limit the miniaturization of devices with such waveguides. The blue dashed line in Fig. 3 shows the scattering loss of a straight waveguide written under the same conditions as for the curved waveguides. Notice that this line crosses that of Eq. (1) at $R = 1.4$ cm, which means that when $R > 1.4$ cm, the primary loss mechanism is the scattering loss inherit to straight waveguides, while when $R < 1.4$ cm bending loss dominates.

To better characterize the curved waveguides written with this method, Fig. 4 shows Raman measurements of the Si material in the vicinity of the $R = 2.5$ cm waveguide cross section (*y*-*z* plane). The sample is cleaved perpendicular to the waveguide. The cross-section of the waveguides was examined under the Raman microscope directly without further processing to avoid any modification of the modified zone. The sample is characterized with a Raman microscope (Renishaw, inVia) at three positions indicated on the inset optical image. The position termed reference signal in Fig. 4 is an unmodified region of the Si sample. This measurement shows the typical Raman features of crystalline Si (c-Si) peaked at 520 cm^{-1}. Two additional measurements were taken within the waveguide cross section, i.e., where the writing laser has modified the material, and are called position 1 and position 2. Here, features representing amorphous Si (a-Si) at 400–500 cm^{-1} are seen along with decreased crystallinity due to the formation of polycrystalline Si (poly-Si) at 510 cm^{-1}. Specifically, the spectrum corresponding to position 1 in Fig. 4 has a slightly asymmetrical shape about 520 cm^{-1}, which could be due to poly-Si (peak at 510 cm^{-1}, slightly below c-Si at 520 cm^{-1}). The spectrum for position 2 shows the signature of a-Si (wide broadening from 400 to 500 cm^{-1}). In principle, one could extract information about the ratio of laser-induced a-Si and poly-Si with respect to c-Si from these measurements [25]. We estimate that a-Si and poly-Si is no more than a few percent of c-Si based on the theory in [25], although a more precise estimate is not obtained here. Nevertheless, these results mean that the inner region of the waveguide consists mostly of c-Si with a small percentage of disturbed crystalline structures and is consistent with previous studies [26,27].

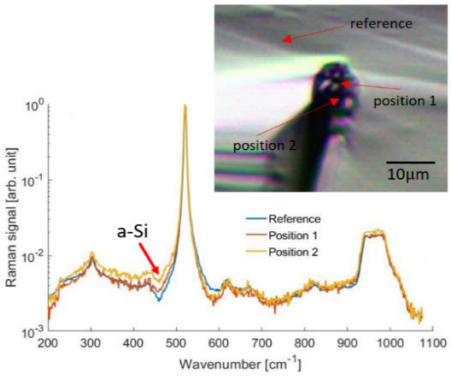

Fig. 4. Raman microscope spectra in the vicinity of a curved waveguide cross section. The different spectra correspond to the positions indicated in the microscope image. The profiles are normalized based on the assumption that the profiles should overlap beyond 1100 cm^{-1}.

4. Conclusion

We have shown a new method to write semicircular curved waveguides of different radii in silicon with a shaped nanosecond laser beam. The bending losses of the waveguides are measured, showing good agreement with the theoretical prediction. For the fabrication conditions used here, the dependence of the bending loss on curvature radius exhibits an approximate exponential decay for radii greater than one cm and a hybrid exponential/power-law increase for radii less than one cm. Raman spectra of the waveguides demonstrate that a small percentage of amorphous and polycrystalline silicon is generated during the writing process. Our work is a step forward towards the goal of a single-step fabrication process of complicated waveguide structures in silicon for telecommunications applications as one example. Yet, our results show that future work is needed to fully develop this new method and write waveguides with more complicated shapes and better performance. In particular, we envision that a better understanding of the physical mechanism of the waveguides formation process will inform future improvements.

Funding. National Science Foundation (NSF) (1903740); National Science Foundation (NSF) (1665456); Air Force Office of Scientific Research (AFOSR) (FA9550-19-1-0078);

Acknowledgments. The authors thank the James R. Macdonald Laboratory of Kansas State University for their assistance.

Disclosures. The authors declare no conflicts of interest.

Data availability. Data underlying the results presented in this paper are not publicly available at this time but may be obtained from the authors upon reasonable request.

References

[1] M. Beresna, M. Gecevicius, and P. G. Kazansky, "Ultrafast laser direct writing and nanostructuring in transparent materials," Adv. Opt. Photonics **6**(3), 293–339 (2014).

[2] Osellame, S. Taccheo, M. Marangoni, R. Ramponi, P. Laporta, D. Polli, S. De Silvestri, and G. Cerullo, "Femtosecond writing of active optical waveguides with astigmatically shaped beams," J. Opt. Soc. Am. B 20, 1559 (2003).

[3] F. Chen and J. R. V. de Aldana, "Optical waveguides in crystalline dielectric materials produced by femtosecond-laser micromachining," Laser Photonics Rev. **8**, 251–275 (2014).

[4] A. Stone, H. Jain, V. Dierolf, M. Sakakura, Y. Shimotsuma, K. Miura, K. Hirao, J. Lapointe, and R. Kashyap, "Direct laser-writing of ferroelectric single-crystal waveguide architectures in glass for 3D integrated optics," Sci. Rep. **5**, 1–10 (2015).

[5] A. H. Nejadmalayeri, P. R. Herman, J. Burghoff, M. Will, S. Nolte, A. Tünnermann, "Inscription of optical waveguides in crystalline silicon by mid-infrared femtosecond laser pulses" Opt. Lett., **30**(9), 964-966 (2005).

[6] P. C. Verburg, G. R. B. E. Römer, and A. J. Huis In 't Veld, "Two-photon-induced internal modification of silicon by erbium-doped fiber laser," Opt. Ex. **22**, 21958–71 (2014).

[7] M. Chambonneau, Q. Li, M. Chanal, N. Sanner, and D. Grojo, "Writing waveguides inside monolithic crystalline silicon with nanosecond laser pulses," Opt. Lett. **41**, 4875 (2016).

[8] X. Yu, X. Wang, M. Chanal, C. A. Trallero-Herrero, D. Grojo, and S. Lei, "Internal modification of intrinsic and doped silicon using infrared nanosecond laser," Appl. Phys. A Mater. Sci. Process. **122**, 1–7 (2016).

[9] X. Wang, X, Yu, H. Shi, X. Xian, M. Chambonneau, D. Grojo, B. DePaola, M. Berg and S. Lei, "Characterization and control of laser induced modification inside silicon" J. Laser Appl. **31**, 022601 (2019).

[10] M. Chambonneau, X. Wang, X. Yu, Q. Li, D. Chaudanson, S. Lei, and D. Grojo, "Positive- and negative-tone structuring of crystalline silicon by laser-assisted chemical etching," Opt. Lett. **44**, 1619 (2019).

[11] H. Kämmer, G. Matthäus, S. Nolte, M. Chanal, O. Utéza, and D. Grojo, “In-volume structuring of silicon using picosecond laser pulses,” Appl. Phys. A Mater. Sci. Process. **124**, 1–6 (2018).

[12] A. Turnali, M. Han, and O. Tokel, “Laser-written depressed-cladding waveguides deep inside bulk silicon,” J. Opt. Soc. Am. B **36**, 966-970 (2019).

[13] O. Tokel, A. Turnall, G. Makey, P. Elahi, T. Çolakoğlu, E. Ergeçen, Ö. Yavuz, R. Hübner, M. Zolfaghari Borra, I. Pavlov, A. Bek, R. Turan, D. K. Kesim, S. Tozburun, S. Ilday, and F. Ö. Ilday, “In-chip microstructures and photonic devices fabricated by nonlinear laser lithography deep inside silicon,” Nat. Photonics **11**, 639–645 (2017).

[14] I. Pavlov, O. Tokel, S. Pavlova, V. Kadan, G. Makey, A. Turnali, Ö. Yavuz, and F. Ö. Ilday, “Femtosecond laser written waveguides deep inside silicon,” Opt. Lett. **42**(15), 3028–3031 (2017).

[15] M. Chanal, V. Y. Fedorov, M. Chambonneau, R. Clady, S. Tzortzakis, and D. Grojo, “Crossing the threshold of ultrafast laser writing in bulk silicon,” Nat. Commun. **8**, 1–6 (2017).

[16] Wang, A., Das, A., & Grojo, D. (2020). Temporal-contrast imperfections as drivers for ultrafast laser modifications in bulk silicon. *Physical Review Research*, *2*(3), 033023.

[17] Y. Cheng, K. Sugioka, K. Midorikawa, M. Masuda, K. Toyoda, M. Kawachi, and K. Shihoyama, "Control of the cross-sectional shape of a hollow microchannel embedded in photostructurable glass by use of a femtosecond laser," Opt. Lett. 28, 55 (2003).

[18] M. Ams, G. D. Marshall, D. J. Spence, and M. J. Withford, “Slit beam shaping method for femtosecond laser direct-write fabrication of symmetric waveguides in bulk glasses,” Opt. Express **13**, 5676-5681 (2005).

[19] A. Yariv and Y. Pochi Photonics: optical electronics in modern communications (Oxford University, 2006).

[20] X. Wang, X, Yu, M. Berg, B. DePaola, H. Shi, P. Chen, L. Xue, X. Chang and S. Lei., “Nanosecond laser writing of straight and curved waveguides in silicon with shaped beams,” J. Laser Appl. **32**(2), 022002 (2020).

[21] D. Marcuse, “Curvature loss formula for optical fibers,” J. Opt. Soc. Am. A **66**(3), 216-220 (1976).

[22] Marcuse, “Bend loss of slab and fiber modes computed with diffraction theory,” IEEE journal of quantum electronics, **29**(12), 2957-2961 (1993).

[23] L. Lewin, Theory of waveguides: Techniques for the solution of waveguide problems, (University of California, 1975).

[24] L. Lewin, D. C. Chang and E. F. Kuester, *Electromagnetic waves and curved structures* (Peregrinus, 1977).

[25] V. G. Golubev, V. Y. Davydov, A. V. Medvedev, A. B. Pevtsov and N. A. Feoktistov, “Raman scattering spectra and electrical conductivity of thin silicon films with a mixed amorphous-nanocrystalline phase composition: Determination of the nanocrystalline volume fraction,” Phys. Solid State, **39**(8), 1197-1201 (1997).

[26] H. Kämmer, G. Matthäus, K. A. Lammers, C. Vetter, M. Chambonneau, and S. Nolte “Origin of waveguiding in ultrashort pulse structured silicon,” Laser Photonics Rev. **13**(2), 1800268 (2019).

[27] Smillie, L. A., M. Niihori, L. Rapp, B. Haberl, J. S. Williams, J. E. Bradby, C. J. Pickard, and A. V. Rode. "Micro-Raman spectroscopy of ultrashort laser induced microexplosion sites in silicon." *arXiv preprint arXiv:2003.14039* (2020).

Chapter 5 - Complex Waveguides in Silicon Written by a Shaped Laser Beam

Abstract

We demonstrate, for the first time, the direct writing of complex optical waveguides in monocrystalline silicon. Straight-curved waveguides are successfully written inside silicon by a pulse nanosecond laser. The loss of the complex waveguides is measured. This direct laser-writing method may advance fabrication capabilities for 3D integrated silicon photonic devices.

1. Introduction

Laser writing of optical waveguides inside dielectrics has been well studied in the past decades [1,2]. The waveguide is formed by generating a refractive-index contrast between the laser-induced structural modifications and the surrounding unmodified regions [3-5]. Two-photon–induced internal modification of Si was studied by Verburg et al. [6]. Investigations of the elongated structures and internal modifications formed by ns laser pulses were reported in [7-10]. Single-mode waveguides written inside Si with ns, ps and fs laser pulses were also demonstrated in [11-15]. Temporal contrast of the ultrashort pulses is proved to be a critical driving parameter in the process of modification formation [16].

There are two commonly used methods to write waveguides, i.e., longitudinal writing and transverse writing [1]. The waveguides lengths are limited to several millimeters in the longitudinal writing because of the shortness of the lens focal distance [7 -15]. On the other hand, the transverse method provides the possibility of writing long waveguides without the restriction of lens working distance. However, the cross-sectional shape of the waveguide is usually asymmetric in the transverse method. Fortunately, this drawback could be overcome by using shaped beams [2,17,18].

The transverse writing method has an advantage in that it provides more flexibility to write waveguide paths with complex shapes. Unlike straight waveguides, the bending loss of curved waveguides cannot be ignored. The theory of bending loss in curved waveguides has been studied in [19-24]. In the year of 1976, Marcuse published the first loss formula for optical fibers with a constant radius of curvature [21].

The possibility of transverse writing of waveguides inside silicon by shaped beams has been reported in our previous work [20]. In this paper, waveguide paths with complicated shapes are studied. The straight-curved waveguides have been successfully written and characterized inside silicon. The waveguides are proved to be able to guide light, and their loss is measured.

2. Experimental Details

To write waveguides with complicated shapes, we will start from a simple one, J-shape. The J-shape waveguide consists of a straight part and a quarter circular part. The silicon wafers used to write the waveguide are intrinsic, (100)-oriented, and 1-mm thick. The resistivity is greater than 200 Ω·cm. The experimental arrangement used for writing is shown in Fig. 1. The wavelength and the pulse duration of the laser (MWTech, PFL-1550) are 1550 nm and 3.5 ns, respectively. The repetition rate is 20-150 kHz and the maximum pulse energy is 20 μJ. The diameter of the output beam is 6 mm. A pair of cylindrical lenses, CL1 and CL2, are used to shape the beam. The distance between the two lenses is $|f_1| - |f_2|$, where f_1(30 cm) and f_2 (-3 cm) are the focal lengths of the two lenses, respectively. A spherically corrected objective lens (Olympus, LCPLN100XIR, NA = 0.85) is used to focus the beam into the silicon sample. At the focal point in the x-z plane, the focal spot size is $2w_0 = 1.22\,\lambda/NA = 2.2$ μm, and the Rayleigh length is z_R = 2.6 μm in air and $z_R \approx$ 9.2 μm in Si. Along the y and z directions, the spot radii are both 9.2 μm.

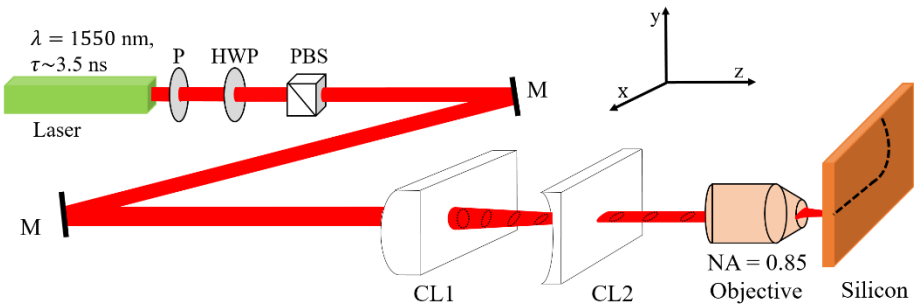

Fig. 1. Experimental arrangement used for transverse writing of waveguides. The combination of a polarizer (P), half-wave plate (HWP), and polarizing beam splitter (PBS) is used to tune the output power. Other optical elements include mirrors (M) and two cylindrical lenses (CL1) and (CL2). A Si wafer sample is mounted on a rotation stage with the rotation axis parallel to the *z*-axis as shown.

The silicon sample in our experiment is mounted on a motorized rotation stage (Newport, SR50PP), which itself is mounted on a XYZ translation stage (Newport, ILS100PP). The laser light is focused at the depth of 0.5 mm. The straight part of the J-shape waveguide is written by moving the sample linearly, while the curved part is written by rotating the silicon sample by 90/180 degrees. The use of the rotation stage ensures that the waveguides are written by the same beam profile.

3. Results and Discussion

To characterize the waveguide, we will measure its numerical aperture (NA) first by coupling into it a CW beam from the λ =1550 nm laser using another microscope objective with $NA = 0.2$, using the setup shown in Fig. 2. The light emerging from the waveguide is then recorded with an InGaAs camera at a distance of L from the waveguide exit. The far-field (L = 2.6 cm) and near-field (L = 3 mm) intensity distributions of light from the waveguide can be measured. The far-field distribution is then fit to a Gaussian profile, yielding a mode waist radius of a. The NA of the waveguide can then be determined by $NA = \frac{a}{L}$. Lastly, by approximating the laser-induced

modification to be step-like in refractive index, we estimate the refractive-index change Δn from NA=$\sqrt{2n\Delta n}$.

Next, we will measure the loss of the waveguides. The damping loss can be calculated by the equation $\alpha = 10 \log (P_1/P_2)/d$, where d, P_1 and P_2 are the waveguide length, input power and output power, respectively. We will measure the input power P_1 at the entrance side of the waveguide and the output power P_2 at the exit side using a power meter. In this calculation, the loss due to the Fresnel reflection at both the front and back face and the coupling loss due to the NA mismatch between the objective lens and the waveguide will be subtracted from the total loss.

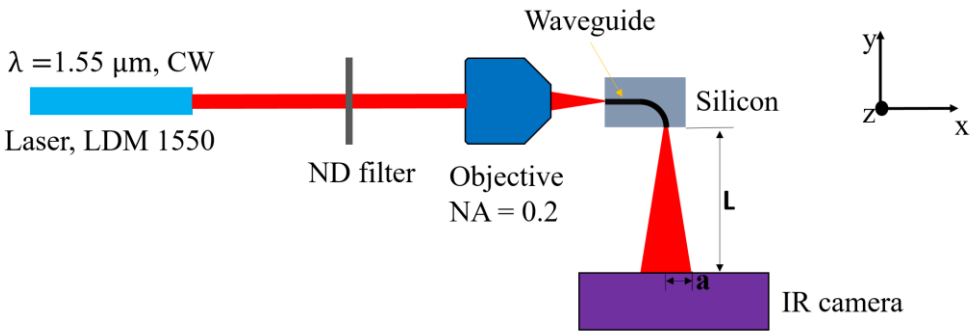

Fig. 2. Experiment setup for characterizing the waveguide.

Fig. 3 shows a waveguide which includes both a straight part and a quarter circle. The length of the straight part is 3 mm and the radius of the quarter circle is 1.5 cm. The input light is coupled into the waveguide from the entrance as the red arrow shows. The light scatters as it travels along a waveguide arc and this scattered light is imaged with an IR camera over a limited field of view. The green arrow shows the joint of straight part and curved part. By stitching together multiple images, a mosaic is formed revealing the entire waveguide arc length. The inset is the far-field image of the output light. The loss of the waveguide is calculated as 4.4 dB/cm and the joint loss is 0.2 dB.

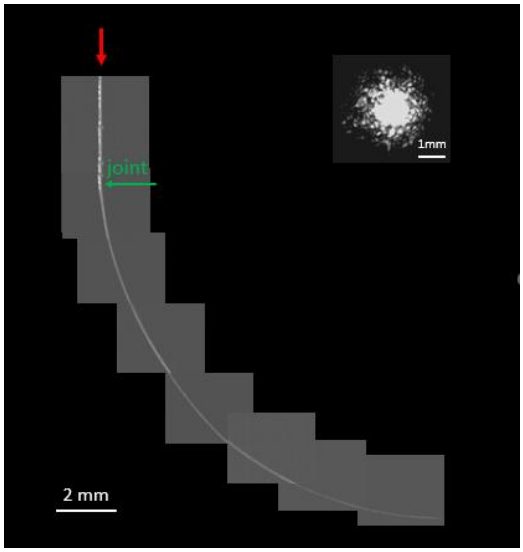

Fig. 3. Straight-quarter circle waveguide. The input light is coupled into the waveguide from the entrance as the red arrow shows. The light scatters as it travels along a waveguide arc and this scattered light is imaged with an IR camera over a limited field of view. By stitching together multiple images, a mosaic is formed revealing the entire waveguide arc length. The inset is the far-field image of the output light.

To have a more complicated shape, we extend the curved part to a half-circle. The length of the straight part is 3 mm and the radius of the curved part is still 1.5 cm. Fig. 4 shows the waveguide. The scatted light of the waveguide proves that the waveguide is able to guide light. The loss of the waveguide is 4.5 dB/cm. And the damping loss is 0.2 dB. This proves the repeatability of our method.

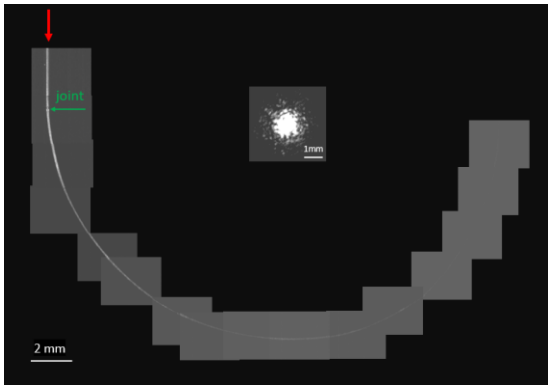

Fig. 4 Straight-half circle waveguide. As in Fig. 3, the input light is coupled into the waveguide from the entrance as the red arrow shows and the inset shows a far-field image of the output light.

4. Conclusions

Straight-curved waveguides with two different circular angles are reported in the paper. The waveguides are proved to be able to guide light. The loss of the waveguides and the joint point between the straight and the curved segments is measured to be 0.2 dB. The waveguides inside silicon are not limited to the mentioned shapes. More complicated shapes will be necessary for higher integration density in the future. Our work is a step forward towards the goal of a single-step fabrication process of complicated waveguide structures in silicon for telecommunications applications as one example. Yet, our results show that future work is needed to write waveguides with more complicated shapes and better performance.

Funding. National Science Foundation (NSF) (2128962, 1665456, 2129006); Air Force Office of Scientific Research (AFOSR) (FA9550-19-1-0078)

Acknowledgments. The authors thank the James R. Macdonald Laboratory of Kansas State University for their assistance.

Disclosures. The authors declare no conflicts of interest.

Data availability. Data underlying the results presented in this paper are not publicly available at this time but may be obtained from the authors upon reasonable request.

References

[1] M. Beresna, M. Gecevicius, and P. G. Kazansky, “Ultrafast laser direct writing and nanostructuring in transparent materials,” Adv. Opt. Photonics 6(3), 293–339 (2014).

[2] R. Osellame, S. Taccheo, M. Marangoni, R. Ramponi, P. Laporta, D. Polli, S. De Silvestri, and G. Cerullo, "Femtosecond writing of active optical waveguides with astigmatically shaped beams," J. Opt. Soc. Am. B 20, 1559 (2003).

[3] F. Chen and J. R. V. de Aldana, “Optical waveguides in crystalline dielectric materials produced by femtosecond-laser micromachining,” Laser Photonics Rev. 8, 251–275 (2014).

[4] A. Stone, H. Jain, V. Dierolf, M. Sakakura, Y. Shimotsuma, K. Miura, K. Hirao, J. Lapointe, and R. Kashyap, “Direct laser-writing of ferroelectric single-crystal waveguide architectures in glass for 3D integrated optics,” Sci. Rep. 5, 1–10 (2015).

[5] A. H. Nejadmalayeri, P. R. Herman, J. Burghoff, M. Will, S. Nolte, A. Tünnermann, “Inscription of optical waveguides in crystalline silicon by mid-infrared femtosecond laser pulses” Opt. Lett., 30(9), 964-966 (2005).

[6] P. C. Verburg, G. R. B. E. Römer, and A. J. Huis, “Two-photon-induced internal modification of silicon by erbium-doped fiber laser,” Opt. Ex. 22, 21958–71 (2014).
[7] M. Chambonneau, Q. Li, M. Chanal, N. Sanner, and D. Grojo, “Writing waveguides inside monolithic crystalline silicon with nanosecond laser pulses,” Opt. Lett. 41, 4875 (2016).
[8] X. Yu, X. Wang, M. Chanal, C. A. Trallero-Herrero, D. Grojo, and S. Lei, “Internal modification of intrinsic and doped silicon using infrared nanosecond laser,” Appl. Phys. A Mater. Sci. Process. 122, 1–7 (2016).
[9] X. Wang, X, Yu, H. Shi, X. Tian, M. Chambonneau, D. Grojo, B. DePaola, M. Berg and S. Lei, “Characterization and control of laser induced modification inside silicon” J. Laser Appl. 31, 022601 (2019).
[10] M. Chambonneau, X. Wang, X. Yu, Q. Li, D. Chaudanson, S. Lei, and D. Grojo, “Positive- and negative-tone structuring of crystalline silicon by laser-assisted chemical etching,” Opt. Lett. 44, 1619 (2019).
[11] H. Kämmer, G. Matthäus, S. Nolte, M. Chanal, O. Utéza, and D. Grojo, “In-volume structuring of silicon using picosecond laser pulses,” Appl. Phys. A Mater. Sci. Process. 124, 1–6 (2018).
[12] A. Turnali, M. Han, and O. Tokel, “Laser-written depressed-cladding waveguides deep inside bulk silicon,” J. Opt. Soc. Am. B 36, 966-970 (2019).
[13] O. Tokel, A. Turnall, G. Makey, P. Elahi, T. Çolakoğlu, E. Ergeçen, Ö. Yavuz, R. Hübner, M. Zolfaghari Borra, I. Pavlov, A. Bek, R. Turan, D. K. Kesim, S. Tozburun, S. Ilday, and F. Ö. Ilday, “In-chip microstructures and photonic devices fabricated by nonlinear laser lithography deep inside silicon,” Nat. Photonics 11, 639–645 (2017).
[14] I. Pavlov, O. Tokel, S. Pavlova, V. Kadan, G. Makey, A. Turnali, Ö. Yavuz, and F. Ö. Ilday, “Femtosecond laser written waveguides deep inside silicon,” Opt. Lett. 42(15), 3028–3031 (2017).
[15] M. Chanal, V. Y. Fedorov, M. Chambonneau, R. Clady, S. Tzortzakis, and D. Grojo, “Crossing the threshold of ultrafast laser writing in bulk silicon,” Nat. Commun. 8, 1–6 (2017).
[16] A. Wang, A. Das, and D. Grojo. (2020). Temporal-contrast imperfections as drivers for ultrafast laser modifications in bulk silicon. Physical Review Research, 2(3), 033023.

[17] Y. Cheng, K. Sugioka, K. Midorikawa, M. Masuda, K. Toyoda, M. Kawachi, and K. Shihoyama, "Control of the cross-sectional shape of a hollow microchannel embedded in photostructurable glass by use of a femtosecond laser," Opt. Lett. 28, 55 (2003).
[18] M. Ams, G. D. Marshall, D. J. Spence, and M. J. Withford, “Slit beam shaping method for femtosecond laser direct-write fabrication of symmetric waveguides in bulk glasses,” Opt. Express 13, 5676-5681 (2005).
[19] A. Yariv and Y. Pochi Photonics: optical electronics in modern communications (Oxford University, 2006).
[20] X. Wang, X, Yu, M. Berg, B. DePaola, H. Shi, P. Chen, L. Xue, X. Chang and S. Lei., “Nanosecond laser writing of straight and curved waveguides in silicon with shaped beams,” J. Laser Appl. 32(2), 022002 (2020).
[21] D. Marcuse, “Curvature loss formula for optical fibers,” J. Opt. Soc. Am. A 66(3), 216-220 (1976).
[22] Marcuse, “Bend loss of slab and fiber modes computed with diffraction theory,” IEEE journal of quantum electronics, 29(12), 2957-2961 (1993).
[23] L. Lewin, Theory of waveguides: Techniques for the solution of waveguide problems, (University of California, 1975).
[24] L. Lewin, D. C. Chang and E. F. Kuester, Electromagnetic waves and curved structures (Peregrinus, 1977).
[25] V. G. Golubev, V. Y. Davydov, A. V. Medvedev, A. B. Pevtsov and N. A. Feoktistov, “Raman scattering spectra and electrical conductivity of thin silicon films with a mixed amorphous-nanocrystalline phase composition: Determination of the nanocrystalline volume fraction,” Phys. Solid State, 39(8), 1197-1201 (1997).
[26] H. Kämmer, G. Matthäus, K. A. Lammers, C. Vetter, M. Chambonneau, and S. Nolte “Origin of waveguiding in ultrashort pulse structured silicon,” Laser Photonics Rev. 13(2), 1800268 (2019).
[27] L. A. Smillie, M. Niihori, L. Rapp, B. Haberl, J. S. Williams, J. E. Bradby, C. J. Pickard, and A. V. Rode. "Micro-Raman spectroscopy of ultrashort laser induced microexplosion sites in silicon." arXiv preprint arXiv:2003.14039 (2020).

Chapter 6 - Structural changes of nanosecond laser modifications inside silicon

Abstract

Structural changes of waveguides written in the bulk of silicon by a nanosecond laser is investigated. Raman and TEM measurements of waveguide cross sections reveal highly localized crystal deformations. Raman results prove the existence of amorphous silicon inside modifications, and the percentage of amorphous silicon is calculated based on the Raman spectrum. For the first time, the HRTEM images directly show the appearance of amorphous silicon inside nanosecond laser induced modification. This may explain the origin of the positive refractive index change associated with the written waveguides. The modifications consist of highly confined regions of silicon with a disturbed crystal structure accompanied with strain.

1. Introduction

Silicon is the most important material in the semiconductor industry and provides the basis for modern optical and electro-optical technologies. One of the prime desires in the communications industry today is the merging of electronic and photonic devices on the same chip [1,2]. In order to achieve this goal, direct writing of optical elements using ultrashort laser pulses is a promising approach [3–5]. However, in contrast to glasses or other dielectrics, direct writing inside silicon involves several difficulties, including strong spherical aberrations and pronounced nonlinear interaction.

Within the last two decades, numerous attempts have been performed to overcome these limitations [9–12]. Localized modifications in the bulk of silicon using ultrashort laser pulses have been demonstrated [13–16]. Direct writing of single-mode waveguides in Si with picosecond laser pulses is demonstrated [21]. Waveguides can also be written using femtosecond (fs) pulses as demonstrated [12], even though the induced modifications are generated only at the SiO_2/Si interface. Waveguides deep into bulk Si are first reported with 350 fs laser pulses at a wavelength

of1550 nm [2324], where a 10^{-4} refractive index change in magnitude is seen. Local modification in bulk Si with sub-100-fs laser pulses is achieved [25], with single pulses tightly focused at the center of silicon spheres using extreme solid-immersion focusing. Besides using ultrashort pulses, longitudinally written waveguides inside silicon by nanosecond laser are reported [17]. Depressed-cladding waveguides inside bulk silicon written by nanosecond laser pulses are achieved [22]. Both straight and curved waveguides are written inside silicon by transverse ns laser writing [19, 31]. Investigations of the properties of the internal modifications generated by nanosecond laser pulses are presented [18–20].

The past decades have seen achievements in the field of laser induced modifications and waveguide writing inside silicon; however, many problems remain to be solved. One problem is related to the structural changes of the modifications inside silicon induced by a pulsed laser. When laser pulses, especially ultrashort pulses, are focused inside silicon, the extreme high temperature and pressure at the focusing spot often result in complicated material changes, such as melting, explosion, shock wave, and resolidification. Past research has shown many different material changes inside silicon induced by pulsed lasers, including voids[26, 27], high pressure phases [28], dislocations [10,29], hydrostatic compressive strain [10,29], cracks [26], and polycrystalline features [13,28,30]. Another problem is concerned with the light guiding mechanism of the waveguides created inside silicon. One could wonder about the origin of the positive refractive index change associated with the written waveguides. Given the higher refractive index of amorphous silicon $n_{a-Si} = 3.73$, compared to the one of crystalline silicon $n_{c-Si} = 3.48$ (at 1.55 μm wavelength), one could expect a partial amorphization of the material for explaining the waveguiding properties [30]. However, there has been no direct evidence showing the amorphous silicon inside nanosecond laser induced modifications and waveguides.

A better understanding of the material changes inside ns laser induced modifications is important to provide guidance for the next generation of silicon devices. It is critical to understand the mechanism of light guiding of the waveguides inside silicon and make low loss waveguides possible.

In this paper, we investigate the structural changes of ns-laser written waveguides in silicon by means of Raman microscopy and TEM. Our Raman results prove the existence of amorphous silicon inside modifications, and the percentage of amorphous silicon is calculated based on the Raman spectrum. For the first time, the HRTEM images directly show the appearance of amorphous silicon inside ns laser induced modifications. Such amorphous silicon may be responsible for a positive refractive index change in the range of 10^{-3}.

2. Experimental setup

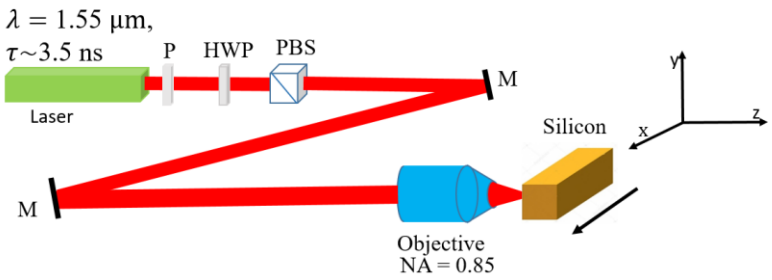

Fig. 1. Experimental setup for transverse ns laser writing inside silicon.

The experimental setup for laser modification inside silicon is shown in Fig 1. The laser is a fiber MOPA (master oscillator power amplifier) laser (MWTechnologies, Model PFL-1550) delivering laser pulses at 1.55 µm center wavelength and 3.5 ns FWHM (full-width-at-half-maximum) pulse duration. The pulse repetition rate is 20-150 kHz and the pulse energy is 20 µJ. During waveguide writing, a spherically corrected objective lens (Olympus, LCPLN100XIR, NA = 0.85) is used to focus the beam into the silicon sample. The focal spot size is $2w_0 = 1.22\,\lambda/NA = 2.2$ µm, and the Rayleigh length is z_R = 2.6 µm in air and $z_R \approx$ 9.2 µm in Si. The relative position between the sample and the objective lens will be controlled using an XYZ translation stage (Newport, ILS100PP). The writing direction is perpendicular to the beam propagation axis. After laser inscription, the sample will be cleaved to observe the cross section of the waveguide by an optical microscope. Raman spectroscopy will be used to determine the composition of the modification. Lamella samples will be prepared from the modification for TEM analysis to reveal the atomic scale microstructure of the modification.

The writing parameters to be changed include pulse energy and pulse repetition rate. The writing speed is fixed at 1 mm/s. The experimental design is shown in Table 1.

Table 1 Nanosecond laser writing conditions.

Pulse Energy (μJ)	Repetition Rate (kHz)
10	20
10	60
10	100
6	20
6	60
6	100
2	20
2	60
2	100

3. Raman Analysis

3.1 Raman spectrum analysis and curve fitting to determine the ratio of the amorphous silicon

In order to investigate the origin of the induced refractive index change, Raman microscopy is applied at a wavelength of 532 nm using a 100× objective with NA = 0.85 (Renishaw inViaRaman microscope). 2D mappings are obtained by scanning with a step size of 1 μm in the x and y directions. The sample is characterized with a Raman microscope at three positions for every modification. An optical image of the cross section of a laser modified zone is shown in Fig. 2, together with the Raman spectrum and the curve-fit Gaussian and Lorentzian components.

One can determine the ratio of the amorphous silicon in the modifications by curve fitting of the Raman spectrum. In the case of silicon with mixed amorphous- monocrystalline phase composition, the spectrum includes a broad low-frequency component peaking around 480 cm^{-1} which is from the amorphous phase, and a narrow peak near 520 cm^{-1} which is from the crystalline phase. The total scattering intensity $I(\omega)$ in the frequency region can be written as

$$I(\omega) = I_c(\omega) + I_a(\omega)$$

where $I_c(\omega)$is the intensity of the line produced by the crystalline phase, and $I_a(\omega)$ is that of the amorphous phase line [32].

3.2 Results of Raman analysis

Based on the above theory, we wrote a python program to analyze the percentage of the amorphous and crystal silicon in the laser induced modifications. The modification in Fig. 2a is written with the pulse repetition rate of 20 kHz, pulse energy of 10 μJ, and scanning speed of 1mm/s. The optical image shows that the modification is not uniform. A heavily modified part in the cross center is found, and the Raman spectrum from this position is analyzed by our self-made program. The results are shown in Fig. 2b. The original Raman data (blue line) are split into two parts, the crystalline part (Lorentzian Component) and the amorphous part (Gaussian component). The analysis is done in python using a fitting module called Non-linear Least-Squares Minimization and Curve-Fitting for Python (Lmfit) [33]. Based on our calculation, the percentage of the amorphous silicon is 50.1% at this location.

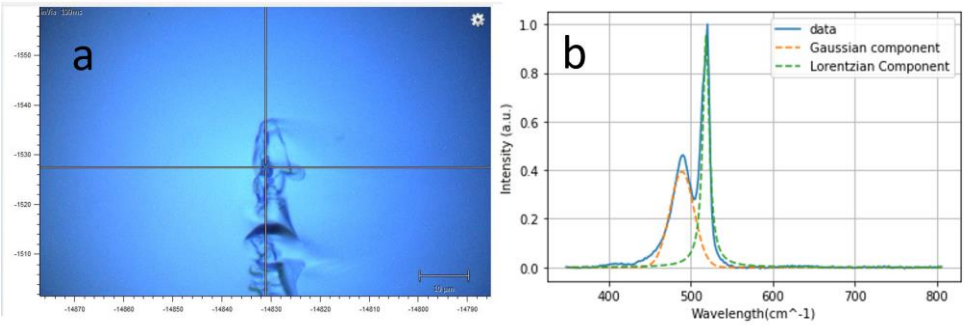

Fig 2. (a) The laser modification inside silicon. (b) The Raman spectrum at the intersect of the two lines in (a). The blue curve is the original data, the orange dashed line is the Gaussian fit (amorphous silicon) and the green dashed line is the Lorentzian fit (monocrystalline silicon).

To better understand the distribution of the amorphous silicon in the modified zone, 2D mapping of the Raman spectrum has been done. Fig. 3a shows the optical image of the modification written with the pulse repetition rate of 20 kHz, pulse energy of 6 μJ, and scanning speed of 1 mm/s. This cross sectional view shows that the modification is elongated and non-uniform. The 2D mapping of the peak intensity at 480 cm^{-1}, an indication of amorphous silicon in the modified zone, is shown in Fig. 3b. The 2D mapping proves that amorphous silicon is created by ns laser writing, but it is non-uniform in the modified zone. A quantitative analysis at each pixel of the

2D mapping produces another 2D mapping, shown in Fig. 3c, for the percentage of amorphous silicon in the modified zone. The highest percentage of the amorphous silicon is about 3%. The samples with other 8 writing conditions also show similar results.

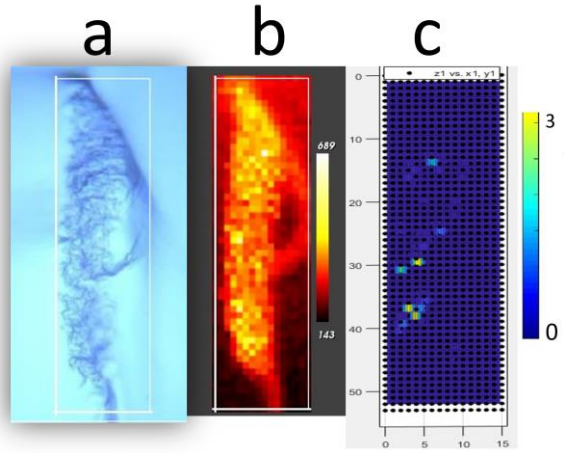

Fig. 3. (a) The optical image of the modified zone under the following conditions: pulse repetition rate=20 kHz, pulse energy=6 μJ, scanning speed=1 mm/s, (b) The intensity distribution of peak 480 cm^{-1}, (c) 2D distribution of the percentage of the amorphous silicon.

4. TEM Analysis

To better characterize the modification in terms of its structural changes, TEM analysis has been done. As illustrated in Fig. 4a, one waveguide is written in the silicon wafer and a lamella is extracted along the x-z plane in the middle of the cross section of the modification. Fig. 4b shows an SEM image of the cross section of the waveguide along the x-y plane and the position of the lamella (in yellow rectangular area). The waveguide is written with a pulse repetition rate of 20 kHz, pulse energy of 10 μJ, and scanning speed of 1mm/s. after removing the surrounding materials by FIB with subsequent thinning, a lamella as shown in Fig. 4c is formed. The lamella is about 10 μm x 10 μm in the x-z plane and about 100 nm thickness in y-direction. Fig. 4d shows the SEM image of the lamella with more details. From Fig. 4c to Fig. 4d, the lamella has been rotated (see the yellow arrow). Fig. 4d shows that the modifications are highly non-uniform. Pockets of severe modifications in dark color seem to appear in random locations against the lighter background, which is in its crystalline form. The long curly thin lines in the upper right

corner and the faint line patterns in other areas are believed to be caused by micro strains. Some cracks can be found in the laser modified region, but it is believed that they are formed after thinning, due to the inherent stress distribution after laser writing. Fig. 4e zooms in on one of the severely modified areas in the lamella. The laser modified region is also observed by high-resolution transmission electron microscopy (HRTEM). Fig. 4f is one example of the TEM results. The material in the Fig. 4f is roughly divided into two parts. The upper part is mainly amorphous silicon and the lower part is mainly crystal silicon. Fig. 4g and 4h are HRTEM images of the red and green rectangular area in Fig. 4f, respectively. The Fig. 4g clearly shows that the atoms of the silicon are randomized. And Fig. 4h shows that the atoms are regular as the original crystal silicon. The inset FFT images of i and j provide solid evidence for the above claim. For the first time, the HRTEM results directly show the appearance of amorphous silicon inside ns laser induced modification.

The amorphous silicon is probably one reason for the light guiding ability of the waveguide, since the refractive index of amorphous silicon is higher than that of the monocrystalline silicon. However, it may not be the only reason, because the amorphous silicon in the modification is not uniform and the percentage is low.

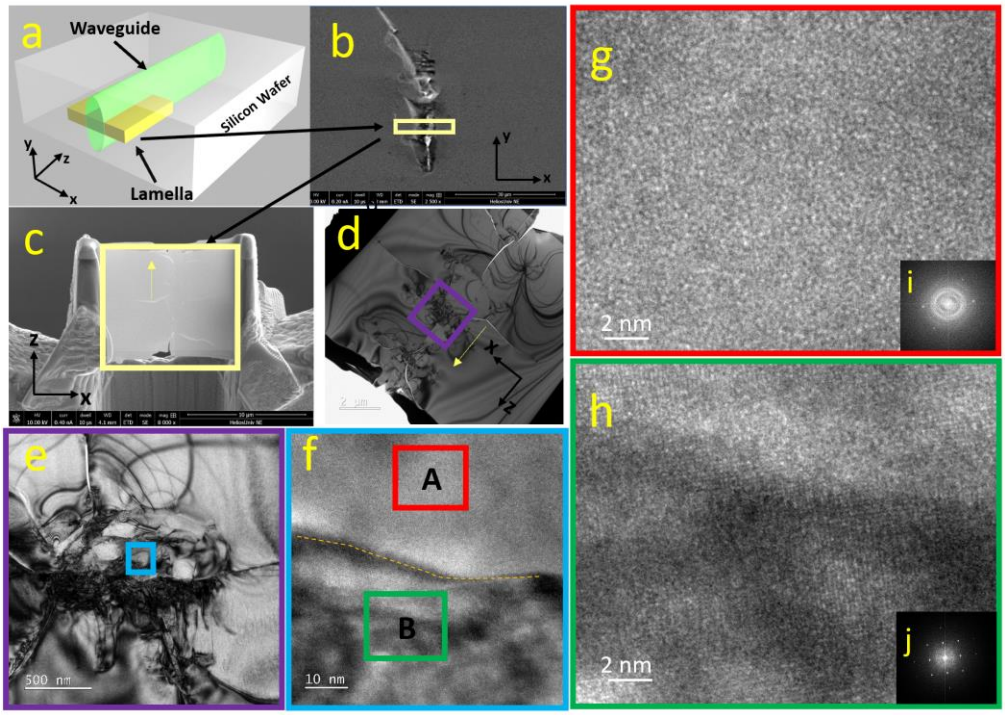

Fig 4. (a) A 3D illustration to show the location of the lamella with respect to the waveguide written inside silicon. (b) The cross section of the waveguide and the location of the lamella (in yellow box). (c) The lamella to be analyzed by TEM. (d, e, f) The TEM image of the modification. (g) The HRTEM image of part A and its corresponding FFT (inset i), (h) The HRTEM image of part B and its corresponding FFT (inset j).

5. Conclusions

We investigated the structural changes of ns laser induced modifications in bulk silicon. This study was performed by Raman microscopy and TEM. The measurements reveal a permanently induced transition from monocrystalline silicon to silicon with disturbed crystal structure. The Raman results prove the existence of amorphous silicon inside modifications and the percentage of the amorphous silicon is calculated based on the Raman spectrum. For the first time, the HRTEM images directly show the appearance of amorphous silicon inside nanosecond laser induced modification. This may explain the origin of the positive refractive index change associated with the ns laser written waveguides. It is believed that the amorphous silicon in combination with

defects are responsible for a positive refractive index change in the range of 10^{-3}. To better understand the material change inside modifications, more experiments with different writing conditions are needed. Our work is a step forward towards the goal of a single-step fabrication process of complicated waveguide structures in silicon for telecommunications applications as one example. Yet, our results show that future work is needed to write waveguides with more complicated shapes and better performance. In particular, we envision that a better understanding of the physical mechanism of the modifications formation process will inform future improvements.

Funding. National Science Foundation (NSF) (2128962, 1665456, 2129006); Air Force Office of Scientific Research (AFOSR) (FA9550-19-1-0078)

Acknowledgments. The authors thank the James R. Macdonald Laboratory of Kansas State University for their assistance.

Disclosures. The authors declare no conflicts of interest.

Data availability. Data underlying the results presented in this paper are not publicly available at this time but may be obtained from the authors upon reasonable request.

References

[1] M. Beresna, M. Gecevicius, and P. G. Kazansky, "Ultrafast laser direct writing and nanostructuring in transparent materials," Adv. Opt. Photonics 6(3), 293–339 (2014).

[2] F. Chen and J. R. V. de Aldana, "Optical waveguides in crystalline dielectric materials produced by femtosecond-laser micromachining," Laser Photonics Rev. 8, 251–275 (2014).

[3] K. Sugioka, "Hybrid femtosecond laser three-dimensional micro-and nanoprocessing: a review," Int. J. Extrem. Manuf. 1, 012003 (2019).

[4] A. Stone, H. Jain, V. Dierolf, M. Sakakura, Y. Shimotsuma, K. Miura, K. Hirao, J. Lapointe, and R. Kashyap, "Direct laser-writing of ferroelectric single-crystal waveguide architectures in glass for 3D integrated optics," Sci. Rep. 5, 1–10 (2015).

[5] A. H. Nejadmalayeri, P. R. Herman, J. Burghoff, M. Will, S. Nolte, A. Tünnermann, "Inscription of optical waveguides in crystalline silicon by mid-infrared femtosecond laser pulses" Opt. Lett., 30(9), 964-966 (2005).

[6] P. C. Verburg, G. R. B. E. Römer, and A. J. Huis In 't Veld, "Two-photon-induced internal modification of silicon by erbium-doped fiber laser," Opt. Ex. 22, 21958–71 (2014).

[7] M. Chambonneau, Q. Li, M. Chanal, N. Sanner, and D. Grojo, "Writing waveguides inside monolithic crystalline silicon with nanosecond laser pulses," Opt. Lett. 41, 4875 (2016).

[8] X. Yu, X. Wang, M. Chanal, C. A. Trallero-Herrero, D. Grojo, and S. Lei, “Internal modification of intrinsic and doped silicon using infrared nanosecond laser,” Appl. Phys. A Mater. Sci. Process. 122, 1–7 (2016).
[9] X. Wang, X, Yu, H. Shi, X. Xian, M. Chambonneau, D. Grojo, B. DePaola, M. Berg and S. Lei, “Characterization and control of laser induced modification inside silicon” J. Laser Appl. 31, 022601 (2019).
[10] M. Chambonneau, X. Wang, X. Yu, Q. Li, D. Chaudanson, S. Lei, and D. Grojo, “Positive- and negative-tone structuring of crystalline silicon by laser-assisted chemical etching,” Opt. Lett. 44, 1619 (2019).
[11] H. Kämmer, G. Matthäus, S. Nolte, M. Chanal, O. Utéza, and D. Grojo, “In-volume structuring of silicon using picosecond laser pulses,” Appl. Phys. A Mater. Sci. Process. 124, 1–6 (2018).
[12] A. Turnali, M. Han, and O. Tokel, “Laser-written depressed-cladding waveguides deep inside bulk silicon,” J. Opt. Soc. Am. B 36, 966-970 (2019).
[13] O. Tokel, A. Turnall, G. Makey, P. Elahi, T. Çolakoğlu, E. Ergeçen, Ö. Yavuz, R. Hübner, M. Zolfaghari Borra, I. Pavlov, A. Bek, R. Turan, D. K. Kesim, S. Tozburun, S. Ilday, and F. Ö. Ilday, “In-chip microstructures and photonic devices fabricated by nonlinear laser lithography deep inside silicon,” Nat. Photonics 11, 639–645 (2017).
[14] I. Pavlov, O. Tokel, S. Pavlova, V. Kadan, G. Makey, A. Turnali, Ö. Yavuz, and F. Ö. Ilday, “Femtosecond laser written waveguides deep inside silicon,” Opt. Lett. 42(15), 3028–3031 (2017).
[15] M. Chanal, V. Y. Fedorov, M. Chambonneau, R. Clady, S. Tzortzakis, and D. Grojo, “Crossing the threshold of ultrafast laser writing in bulk silicon,” Nat. Commun. 8, 1–6 (2017).
[16] M. Ams, G. D. Marshall, D. J. Spence, and M. J. Withford, “Slit beam shaping method for femtosecond laser direct-write fabrication of symmetric waveguides in bulk glasses,” Opt. Express 13, 5676-5681 (2005).
[17] G. Cerullo, R. Osellame, S. Taccheo, M. Marangoni, D. Polli, R. Ramponi, P. Laporta, and S. De Silvestri, “Femtosecond micromachining of symmetric waveguides at 1.5 μm by astigmatic beam focusing.” Opt. Lett., 27(21), 1938-1940 (2002).
[18] A. Yariv and Y. Pochi Photonics: optical electronics in modern communications (Oxford University Press, 2006).

[19] X. Wang, X. Yu, M. Berg, B. DePaola, H. Shi, P. Chen, L. Xue, X. Chang and S. Lei., "Nanosecond laser writing of straight and curved waveguides in silicon with shaped beams," J. Laser Appl. 32(2), 022002 (2020).
[20] D. Marcuse, "Curvature loss formula for optical fibers," J. Opt. Soc. Am. A 66(3), 216-220 (1976).
[21] R. T. Schermer and J. H. Cole, "Improved bend loss formula verified for optical fiber by simulation and experiment," IEEE Journal of Quantum Electronics, 43(10), 899-909 (2007).
[22] D. Marcuse, "Bend loss of slab and fiber modes computed with diffraction theory," IEEE journal of quantum electronics, 29(12), 2957-2961 (1993).
[23] L. Lewin, Theory of waveguides: Techniques for the solution of waveguide problems, (University of California, 1975).
[24] L. Lewin, D. C. Chang and E. F. Kuester, Electromagnetic waves and curved structures (Peregrinus, 1977).
[25] A. H. Nejadmalayeri, P. R. Herman, J. Burghoff, M. Will, S. Nolte, S. and A. Tünnermann, "Inscription of optical waveguides in crystalline silicon by mid-infrared femtosecond laser pulses," Opt. Lett. 30(9), 964-966 (2005).
[26] H. Iwata, D. Kawaguchi, H. Saka, Microscopy 2017, 66, 328.
[27] K. Shimamura, J. Okuma, S. Ohmura, F. Shimojo, J. Phys. Conf. Ser. 2012, 402, 012044.
28. H. Iwata, D. Kawaguchi, H. Saka, Microscopy 2018, 67, 30.
[29] H. Saka, H. Iwata, D. Kawaguchi, Microscopy 2018, 67, 112.
[30] Chambonneau, M., Grojo, D., Tokel, O., Ilday, F. Ö., Tzortzakis, S., & Nolte, S. (2021). In-Volume Laser Direct Writing of Silicon—Challenges and Opportunities. Laser & Photonics Reviews, 15(11), 2100140.
[31] X. Wang, X.Yu, M. Berg, P. Chen, B. Lacroix, S. Fathpour & S. Lei. (2021). Curved waveguides in silicon written by a shaped laser beam. Optics Express, 29(10), 14201-14207.
[32] V. G. Golubev, V. Y. Davydov, A. V. Medvedev, A. B. Pevtsov, and N. A. Feoktistov, "Raman scattering spectra and electrical conductivity of thin silicon films with a mixed amorphous-nanocrystalline phase composition: Determination of the nanocrystalline volume fraction," Phys. Solid State **39**(8), 1197–1201 (1997).

Chapter 7 - Summary and Outlook

This dissertation tries to answer this question about how to take advantage of the laser to make modifications inside silicon and how to extend the modifications into meaningful devices such as waveguides. The dissertation studies the fundamental process of the laser-matter interaction and the material change inside silicon. It is shown that a better understanding of laser-matter interaction is important for developing novel laser processing techniques.

The major achievements of this dissertation are the following:

We generate permanent modifications inside silicon by tightly focusing and continuously scanning the laser beam inside samples, without damaging the front and back surface. Cross sections of these modifications are observed after cleaving the samples and are further analyzed after mechanical polishing followed by chemical etching. The shape of the modification is found to depend on the input beam shape, laser power, and scanning speed.

We demonstrate a method for transverse writing of optical waveguides in a crystalline silicon wafer using a nanosecond laser with a shaped beam profile that is formed by a pair of cylindrical lenses. In contrast to traditional writing methods, this method avoids forming asymmetric waveguide profiles. Both straight and curved waveguides are written with a nearly circular transverse guide-profile and are found to support single-mode propagation for 1550 nm wavelength light.

We demonstrate, for the first time, the direct writing of curved optical waveguides in monocrystalline silicon with different curve radii. The bending loss of the curved waveguides is measured and a good agreement with theoretical values is found. Raman spectroscopy measurements suggest the formation of inhomogeneous amorphous and polycrystalline phases in the laser-modified region.

We write straight-curved waveguides with different angles. The waveguides are proved to be able to guide light. The loss of the waveguides and that at the connection point between the straight and curved portions are measured. The waveguides inside silicon are not limited to the mentioned shapes. More complicated shapes will be necessary for higher integration density in the future.

We investigate the structural changes of ns laser induced modifications in bulk silicon. This study is performed by Raman microscopy and TEM. The measurements reveal a permanently induced transition from monocrystalline silicon to silicon with disturbed crystal structure. The Raman results prove the existence of amorphous silicon inside modifications. The percentage of the amorphous silicon is calculated based on the Raman spectrum, which is location dependent and ranges from 0 to 50%. For the first time, the HRTEM images directly show the appearance of amorphous silicon inside nanosecond laser induced modification. This may explain the origin of the positive refractive index change associated with the ns laser written waveguides.

Our work is a step forward towards the goal of a single-step fabrication process of complicated waveguide structures in silicon for telecommunications applications as one example. Our results

show that future work is needed to fully develop this new method and write waveguides with more complicated shapes and better performance. In particular, we envision that a better understanding of the physical mechanism of the waveguide formation process will inform future improvements.

Recommendations for future work:

How to get uniform modifications? The modifications in the previous work are mostly non-uniform. Uniform modifications are important to get waveguides with lower loss.

How to control the refractive index of the waveguides inside silicon? There is no doubt that the writing conditions and the material have important effects on the refractive index. The previous work just measures the loss of the waveguide and calculates the refractive index of the waveguides after finishing. Rarely work has been reported how to control the refractive index.

Appendix A - List of Publications

1, Mohammad Najjartabar Bisheh, **Xinya Wang**, Shing I. Chang, Shuting Lei & Jianfeng Ma. "Image-based characterization of laser scribing quality using transfer learning". **Journal of Intelligent Manufacturing**,(2022): 1-13.

2, **Xinya Wang**, Xiaoming Yu, Matthew Berg, Pingping Chen, Brice Lacroix, Shuting Lei ,"Curved Waveguides in Silicon Written by a Shaped Laser Beam". ***Optics Express*** 29(10), 14201-14207.

3, Pingping Chen, **Xinya Wang**, Y. Luan, Zhe Fei, Brice Lacroix, Shuting Lei, and Suprem R. Das. "High-field electromagnetic radiation converts carbon nanotubes to nanoribbons embedded with carbon nanocrystals." ***Journal of Applied Physics*** 128, no. 2 (2020): 024305.

4, **Xinya Wang**, Xiaoming Yu, Matthew Berg, Brett DePaola, Hongyu Shi, Pingping Chen, Lianjie Xue, Xuefeng Chang, and Shuting Lei. "Nanosecond laser writing of straight and curved waveguides in silicon with shaped beams." ***Journal of Laser Applications*** 32, no. 2 (2020): 022002.

5, **Xinya Wang**, Xiaoming Yu, Hongyu Shi, Xianhua Tian, Maxime Chambonneau, David Grojo, Brett Depaola, Matthew Berg, and Shuting Lei. "Characterization and control of laser induced modification inside silicon." ***Journal of Laser Applications*** 31, no. 2 (2019): 022601.

6, Chambonneau, M., **Wang, X**., Yu, X., Li, Q., Chaudanson, D., Lei, S., & Grojo, D. (2019). Positive-and negative-tone structuring of crystalline silicon by laser-assisted chemical etching. ***Optics letters***, *44*(7), 1619-1622.

7, Xianhua Tian, Jun Zhao, **Xinya Wang**, Haifeng Yang, Zhongbin Wang. "Performance of Si_3N_4/(W, Ti)C graded ceramic tool in high-speed turning iron-based superalloys", ***Ceramics International***, 44-13, 15579 (2018)

8, Adam Summers, Xiaoming Yu, **Xinya Wang**, Maxime Raoul, Josh Nelson, Daniel Todd, Stefan Zigo, Shuting Lei, and Carlos A. Trallero-Herrero, "Spatial characterization of Bessel-like beams for strong-field physics," ***Optics Express*** 25, 1646-1655 (2017).

9, Xiaoming Yu, **Xinya Wang**, Margaux Chanal, Carlos A Trallero-Herrero, David Grojo, Shuting Lei, "Internal modification of intrinsic and doped silicon using infrared nanosecond laser", ***Applied Physics A***, 122:1001(2016)

10, Wenying Liao, Wande Fan, Yuan Li, Jun Chen, Fanhua Bu, Haipeng Li, **Xinya Wang**, Ding-Ming Huang, "Investigation of a novel all-solid large-mode-area photonic quasi-crystal fiber," ***Acta Physica Sinica*** 034206(2014)

11, Shuting Lei, Guang Yang, **Xinya Wang**, Shouyuan Chen, Amy Prieb, and Jianfeng Ma. "High energy femtosecond laser peening of 2024 aluminum alloy." 10th CIRP Conference on Photonic Technologies Procedia CIRP 74 (2018): 357-361.

12, Xiaoming Yu, **Xinya Wang**, Margaux Chanal, Carlos A Trallero-Herrero, David Grojo, Shuting Lei, “Laser material processing based on non-conventional beam focusing strategies”, *9th International Conference on Photonic Technologies LANE 2016*

13, Adam M. Summers, Jan Tross, Xiaoming Yu, **Xinya Wang**, Shuting Lei, Carlos A. Trallero-Herrero, “Characterization of Bessel-Gauss beams for applications to high harmonic generation”, *Division of Atomic Molecular and Optical Physics 2018*

14, Shuting Lei, **Xinya Wang**, and Jon T. Larsen. "Numerical modeling and simulation of ultrafast laser-matter interaction with aluminum thin film." Procedia CIRP 111 (2022): 571-575.